INFORMATION TO USERS

This manuscript has been reproduced from the microfilm master. UMI films the text directly from the original or copy submitted. Thus, some thesis and dissertation copies are in typewriter face, while others may be from any type of computer printer.

The quality of this reproduction is dependent upon the quality of the copy submitted. Broken or indistinct print, colored or poor quality illustrations and photographs, print bleedthrough, substandard margins, and improper alignment can adversely affect reproduction.

In the unlikely event that the author did not send UMI a complete manuscript and there are missing pages, these will be noted. Also, if unauthorized copyright material had to be removed, a note will indicate the deletion.

Oversize materials (e.g., maps, drawings, charts) are reproduced by sectioning the original, beginning at the upper left-hand corner and continuing from left to right in equal sections with small overlaps.

Photographs included in the original manuscript have been reproduced xerographically in this copy. Higher quality 6" x 9" black and white photographic prints are available for any photographs or illustrations appearing in this copy for an additional charge. Contact UMI directly to order.

ProQuest Information and Learning
300 North Zeeb Road, Ann Arbor, MI 48106-1346 USA
800-521-0600

Université d'Ottawa · University of Ottawa

CHEMORESISTANCE IN HUMAN CANCER CELL LINES: AN INVESTIGATION OF ACTIVE AND PASSIVE RESISTANCE MECHANISMS AND THEIR EFFECT ON THE DOSE-RESPONSE CURVE OF CISPLATIN

by

Mark Adel Nassim

This thesis is submitted in partial fulfillment

of the M.Sc. program in Pharmacology

Cancer Care Ontario
Ottawa Regional Cancer Centre
503 Smyth Road
Ottawa, Ontario K1H 1C4
Canada

&

Cellular and Molecular Medicine
Faculty of Medicine, University of Ottawa
451 Smyth Road
Ottawa, Ontario K1H 8M5
Canada

Monday January 15, 2001

TABLE OF CONTENTS

DEDICATION

Dear Reader,

If you are reading this part of my manuscript, truly you are dedicated and thus let me start off by dedicating my work to you and other investigators who continue to make a difference in the realm of science and the pursuit of truth.

There are others, of course, to whom I would like to dedicate my work. The first person that springs to mind is my grandmother who died of breast cancer at a time when chemotherapy was not as easily tolerated with today's anti-emetics, and the chances of survival were significantly lower than they are now. It is largely my experience of her death that sparked my determination in scientific research, especially in oncology.

I would like to dedicate this work to my parents, Hoda and Adel, as well as my sister Tania, and my brother in law, Michael. They have been a tremendous support as I worked through my third consecutive university degree (trust me guys, it was no big deal, really!).

I would like to also dedicate this work to the scientists, professors and individuals who have had an equally important impact in my life, in both a positive and a negative sense (there are learning experiences to be had everywhere, n'est pas?). I would like to particularly recognize Dr. David Stewart as he has, unconsciously, provided a sense of

what I feel a true physician to be, and I have the utmost respect and appreciation for the impact he has had on my life over the last seven years. Thank you for giving me the opportunity to explore my interests. I would also like to thank Dr. Goel, who has been an equally staunch supporter of all of my endeavours, professionally, academically and philosophically. Both of you have my undying gratitude and friendship.

I would also like to thank Caroline Obeid, my fiancée, who has given me her unflagging support and love over the last 3.7 years, during my continued paradoxical pursuits of enlightenment and understanding via a higher education. Thanks to her, the world is a brighter place which I have learned to even more fully enjoy, all the while maintaining my academic enjoyment and performance. Thanks Caroline!

Finally, I would like to thank the forces that drive me on a daily basis to aspire to my highest potential. I am truly grateful for all of the opportunities I have been given, and can only hope to one day give a little something back to a world, a God, who has been so generous.

OK, consider yourselves warned!

Mark Adel Nassim

ACKNOWLEDGEMENTS

I would like to acknowledge the following individuals for their support and assistance throughout my research work, of which a portion has evolved into this thesis:

Dr. David J. Stewart, for his support and assistance (academically, technically and professionally) throughout my research career, as well as Dr. Rakesh Goel. I would also like to thank Dr. Peter G. Raaphorst, Dr. Chen Ng and Dr. Michael M. McBurney (as well as their technicians, students and staff) for the generous use of their lab facilities. I extend my thanks to Dr. Art Beaubien for his statistical insights, and to Dr. Filion for his training and the use his flow cytometric equipment. I would also like to thank Dr. Srabani Banerjee for her technical assistance, as well as the Ottawa Regional Cancer Centre for use of their facilities, which I have "exploited" since 1994. I have really enjoyed my stay.

I would also like to thank the National Sciences and Engineering and Research Council as well as the University of Ottawa for their numerous scholarships.

I would like to thank Dr. Okaichi (Nagasaki University School of Medicine, Japan) and Dr. Nishio (National Cancer Center Research Institute, Japan) for their generous donation of the Saos-2 and SBC-3 cell lines (and their transfectants), respectively. I would also like to thank Dr. Kondo (Atomic Bomb Disease Institute, Japan) for his generous donation of the γ-GCS_h antibody.

LIST OF TABLES

LIST OF FIGURES

ABBREVIATIONS

AR	active resistance
cDNA	complementary DNA
DMEM	Dulbecco's modified essential medium
DDW	distilled deionised water
DNA	Deoxyribonucleic acid
ELISA	enzyme-linked Immunosorbant assay
G418	Geneticin™
γ-GCS	γ-glutamylcysteine synthetase
GSH	Glutathione
GSSG	glutathione disulphide
GS-X	glutathione-S-conjugate
IPTG	Isopropylthio-β-D-galactoside
kDA	Kilodalton
LD_{50}	lethal dose for 50% of the cell population
MDR	multi-drug resistance
MTX	Methotrexate
PBS	phosphate-buffered saline
PALA	N-phosphonacetyl-L-aspartic acid
PCNA	proliferating cell nuclear antigen
Pi	Phosphate
PR	passive resistance
RB	Retinoblastoma
RNA	ribonucleic acid
Saos-2	human osteosarcoma cell line(devoid of endogenous p53)
Saos-2/p53-	human osteosarcoma cell line transfected with wild-type p53, and selected for non p53-expressing transfectants via long-term exposure to IPTG

Saps-2/p53	human osteosarcoma cell line transfected with wild-type p53
SBC-3	human small-cell lung cancer cell line
SBC-3/GCS	human small-cell lung cancer cell line transfected with γ-GCS
SDS	sodium dodecyl sulfate
SDS-PAGE	sodium dodecyl sulfate polyacrylamide gel electrophoresis
TBS	tris-buffered saline
TBS-T	tris-buffered saline + 10% Tween
w/t	wild-type

ABSTRACT

The shape of the dose-response curve (DRC) has been hypothesized to reflect mechanisms of resistance (Stewart *et al.* Invest. New Drugs 14:115, 1996). Active resistance (AR) would give rise to a shoulder on a DRC, while passive resistance (PR) would result in a reduced slope or terminal plateau. We obtained DRCs for human small cell lung cancer cells (SBC-3), and for human osteosarcoma cells (Saos-2) exposed to cisplatin (1 hour CP [0.02-40 μg/ml]). We then fit the data to curve models using non-linear regression techniques. We repeated this technique with SBC-3 cells transfected with a γ-glutamylcysteine synthetase (γ-GCS) gene, and with Saos-2 cells transfected with a wild-type p53 gene in order to observe their effects on cisplatin resistance. We also repeated these experiments in Saos-2/p53 transfectants whose wild-type p53 production was effectively eliminated, and in SBC-3 and SBC-3/GCS transfectants whose glutathione production was inhibited. RESULTS: Curve modeling of the transfected and parent SBC-3 cell lines suggest that there is a significant difference when the γ-GCS gene is transfected into this cell line, with changes occurring in the LD_{50} and the slope after 1 hour exposure ($p<0.001$ in both cases). A statistically significant difference is also detected between the transfected and parent Saos-2 cells, where the wild-type p53 gene results in a decrease in the terminal plateau, and a subsequent decrease in PR ($p<0.001$). Reversal of the effects of transfection results in an approximate return of the response curve shape to that of the parent cell lines. CONCLUSIONS: Our results suggest that drug resistance mechanisms exert an effect on the shape of the dose-response curve.

1. INTRODUCTION

1.1 The problem of cancer

Cancer accounts for 27% of all Canadian mortality, is the leading cause of premature death, and is the highest single cause of death in both Canadian men and women. It is estimated that 132 100 new cases of cancer and 65 000 deaths from cancer will occur in Canada in 2000 (Canadian Cancer Statistics, 2000). Although primarily a disease of older Canadians, with 70% of new cancer cases and 82% of deaths due to cancer occurring among those at least 60 years old, cancer is the second highest cause of death following trauma in youths. Over their lifetimes, 40% of men, and 35% of Canadian women will be diagnosed with cancer. Conversely, total spending on cancer treatment and research is less than half that of cardiovascular disease, and is also less than that of respiratory or digestive diseases (Canadian Cancer Statistics, 2000).

Surgery continues to be the most effective curative treatment for early stage neoplastic disease, followed by radiotherapy. For the treatment of advanced metastatic disease, chemotherapy (the treatment of cancer with cytotoxic agents) is often the treatment of choice. The improvement of chemotherapeutic approaches is, however, imperative as these modalities yield a wide range of response rates (e.g., colorectal therapy using 5-fluorouracil yields response rates ranging from 10% to 24% [Nassim *et al.*, 1998a]). Of note, however, is that testicular cancer is now as curable as some bacterial infections, and only one third of breast cancer patients end up dying from breast cancer (Canadian Cancer Statistics, 2000). While these figures are an improvement compared to response rates achieved in the past, overall outcome remains poor for most

cancer patients with metastatic disease. Consequently, a focus on the understanding of the various mechanisms behind low response rates, and an investigation into their improvement, is of great interest to clinicians and researchers in medical science. Note that "cure" is arbitrarily considered to be 5 years of complete remission, where the potential for curable cancer depends on the biology of the disease (i.e. breast cancer is never considered as being a curable disease, since it may recur after the initial diagnosis).

Given the tremendous advances in cancer management, as well as the challenge of improving current treatment of this disease, considerable interest and resources have been devoted to this effort. Explorations into the improvement of current therapies and the development of new strategies have resulted in many innovations, including gene therapy, drug biomodulation, immunotherapy, and oligonucleotide therapy (Roth & Cristiano, 1997; Schmitt & Loew, 1999; Volm *et al.*, 1998). The clinical applications of these new approaches have yet to be established, however, as many of them are still in the initial stages of development, and present tentative results at best.

1.2 Drug resistance

While many factors contribute to low response rates, resistance to chemotherapy is a major source of failure in cancer treatment, where normal cells would be wiped out at the cytotoxic concentrations required to eliminate a cancer cell population, or the cytotoxic concentrations necessary to eliminate cancer cells simply cannot be achieved (Volm *et al.*, 1998). Cancer resistance is attributable to many causes at macroscopic, cellular, and molecular levels, and include pharmacokinetic variables, oncotic pressure,

decreased red blood cell deformability, endothelial permeability, tumour vascularity, and protein concentrations in interstitial spaces (Beck and Dalton, 1997). Cellular causes of drug resistance include drug influx/efflux, cytoplasmic factors for drug activation/inactivation, and changes in the molecular target of the drug (e.g. amount of target present, altered target etc.) (Beck and Dalton, 1997).

The majority of cancer chemotherapy drugs mediate cytotoxicity by the inhibition of DNA synthesis, or damage to the DNA template. While tumour cells are thought to be more sensitive than normal cells to such compounds as they frequently synthesise DNA, paradoxically, they may be more resistant to agents whose profile fit these mechanisms of action (Kinsella, 1997). Much of this resistance is developed by the cancer cell upon transformation (Volm, 1998), and could arise from gene amplification (Kinsella, 1997), or the presence of multiple genetic abnormalities (e.g., the activation of oncogenes) (Komiya *et al.*, 1997). The formation of drug resistance at the cellular level has been categorized in many different ways, such as those mechanisms that limit the extent of drug-induced damage, and mechanisms that alter the cellular response to drug-induced damage (Perez, 1998). Other investigators consider drug resistance as either intrinsic or acquired, where intrinsic resistance is defined as a lack of response to anticancer drugs from the outset of a chemotherapeutic regimen (common in solid tumours such as hepatocellular carcinomas and adenocarcinomas of the colon and kidney) (Fardel, 1996). Acquired resistance would involve an initial sensitivity to antitumour drugs, with cells becoming progressively more refractory with repeated drug exposure (e.g. leukaemias and lymphomas) (Fardel, 1996).

Many factors contribute to both acquired and intrinsic resistance. These factors are frequently related to the biochemical features of tumour cells (e.g. drug uptake, drug activation, alteration of target enzyme [e.g. topoisomerase I/II], enhanced expression of detoxifying enzymes ([e.g. glutathione S-transferases] and increased drug efflux.) (Beck & Dalton; Fardel, 1996; Sheikh & Fòrnace, 2000). Other mechanisms include a change in the tolerance of damage to the target (e.g. the ability to synthesise DNA adducts, the disabling of apoptotic pathways, or an alternation in enzyme systems) (Perez, 1998). Changes in these various factors may lead to resistance to more than one agent, and this is referred to as multi-drug resistance (MDR). For instance, enhanced drug efflux can lead to MDR and thus cross-resistance to a broad spectrum of unrelated cancer drugs. This phenomenon has been linked to the overexpression of P-glycoprotein (P-gp) (Beck & Dalton, 1997; Fardel, 1996). Of interest is that cross-resistance between different, structurally similar, cytostatic agents is common amongst anti-cancer drugs (Volm, 1998).

1.3 Active vs. passive resistance

Stewart *et al.* (1996) have proposed an approach to operationally define drug resistance mechanisms as either active or passive resistance. This proposal is the central topic of this thesis, and will be further clarified and discussed in the following pages. According to this classification, resistance mechanisms that arise out of the increased presence or the *de novo* expression of a protective substance, or that are due to the increased activity of a mechanism within the cell, would be classified as active resistance.

Passive resistance would be classified as those types of resistance that arise as a result of the loss of or deficiency in or mutation of a factor.

1.31 Types of active resistance

Gene up regulation, or overexpression, could be involved in the development of active resistance, and might thus arise out of an increase in a number of different gene products. These changes could lead to increases in the quantity or activity of a drug efflux pump (e.g. for glutathione conjugates, multi-resistance protein, p-glycoprotein), an increase in the cell's ability to sequester a drug, or an increase in sulfhydryl inactivation (e.g. by glutathione and other mechanisms mediated by metalloproteins [Shen *et al.*, 1997; Zhang *et al.*, 1998]). Other mechanisms of active resistance could include an increase in the expression of drug-catabolizing enzymes, increased activity in salvage pathways, or an increased expression of DNA repair enzymes.

1.32 Types of passive resistance

Passive resistance might arise due to gene mutation(s), rearrangement, deletion, or down regulation. Some resistance mechanisms that could therefore be classified as passive include deficiencies in cell membrane permeability (e.g. due to decreases in the expression of transport proteins and membrane-specific lipids), or a decrease in the expression of drug anabolizing enzymes (resulting in a decrease of active drug metabolites). Other mechanisms of passive resistance could include a decrease/alteration in the drug target (e.g. deficient topoisomerase I/II, tubulin, or p53 protein), or a

decrease/alteration of necessary cofactors (e.g. reduction of available oxygen in the case of tissue hypoxia) (Stewart *et al.*, 1996). Cells that were deficient in a drug target, or cells in which that drug target was altered such that it was no longer a suitable substrate for the drug, would therefore present a resistant phenotype. For instance, cells that had a decrease in topoisomerase II activity might present a more resistant phenotype to drugs whose obligate target was topoisomerase II (e.g. doxorubicin or etoposide). A similar resistance profile might be observed in cells whose topoisomerase II enzyme had undergone a change at the molecular level that reduced its activity, or changed its binding site thus reducing its affinity for the drug.

1.33 Drug resistance and the dose-response relationship *in vitro*

In the case of chemotherapy, a linear relationship rarely exists between the percentage of a tumour cell population that survives drug exposure and the escalating dosage of a particular drug. It has recently been postulated that the pattern by which drug toxicity varies as the dose is escalated may provide clues as to the most likely mechanisms of tumour cell resistance to that drug and may thereby suggest ways of altering drug administration to optimize efficacy (Stewart *et al.*, 1996). By investigating the effects of an anti-cancer drug on the percent survival of cloned colonies of neoplastic cells, it is possible to construct a drug-sensitivity profile for a particular cell line, termed a dose-response curve. Many studies have confirmed the intuition that fewer cancer cells will survive higher doses of a particular drug (e.g. Raaphorst *et al.*, 1995). The precise shape of the dose-response curve, however, is unpredictable, and few researchers have investigated the possibility of a correlation between the dose-response curve shape and

the classification of resistance mechanisms, a relationship for which only preliminary data are available (Nassim *et al.*, 1998b; Nassim *et al.*, 1997). While a linear dose-response relationship would suggest that a cancer cell population could be completely and predictably destroyed at high doses of anti-cancer agents, a dose-response curve is typically non-linear and may frequently be defined by multiple slopes and inflection points (Nassim *et al.*, 1998b; Nassim *et al.*, 1997). As stated by Stewart and co-authors (1996), the shape of the dose-response curve may not only indicate that a cell possesses a resistance mechanism, but may also indicate which resistance mechanisms the cell uses at differing concentrations of the same drug. Determining the nature of the dose-response relationship may therefore offer some insights into the type of resistance that limits the efficacy of chemotherapy, and might suggest potential resistance modulating strategies.

1.34 Effect of active-passive resistance on the dose-response curve

If a tumour cell population were exposed to a drug to which it was quite sensitive, one would expect a curve type as illustrated in Figure 1A (dotted line). Note that while most pharmacodynamic studies plot *linear* effect versus *log* dose, chemotherapy and radiotherapy cytotoxicity studies instead often plot *log* effect versus *linear* dose. Hence, cytotoxicity curve shapes differ from the usual sigmoid curve of other pharmacodynamic studies (Stewart *et al.*, 1996). Although the trend to graph a dose-response curve with *log* effect vs. *linear* dose is based on convention, it also provides an important advantage from the point of view of cancer chemotherapy. The nature of cancer is such that the most resistant fraction of cells survives following systemic treatment, and it is this persistent, resistant fraction that remains to the detriment of the patient. It is also this

surviving population that may, ultimately, prove to be fatal during subsequent courses of treatment (Stewart *et al.*, 1996). Thus, the resistant fraction of surviving colonies in a dose-response curve represents the real challenge to effective cancer chemotherapy, and it is therefore important to be able to scrutinize any changes in this surviving fraction. Plotting the data as log effect versus linear dose facilitates these observations.

Stewart *et al.* (1996) hypothesized that deviations from the curve presented in Figure 1 (straight, dashed line) correlate with the presence of active or passive resistance mechanisms. Active resistance would give a shoulder on the dose-response curve, with cells resisting the cytotoxic effects of cancer drugs until their resistance mechanisms were overwhelmed or saturated by the increasing concentration of drug (Figure 1A). Saturable passive resistance would be characterized as a sharp drop in the percentage of cell survival after exposure to a drug at low concentrations, followed by a reduced slope or a terminal plateau as the targets of drug action within the cell were exhausted or saturated (Figure 1B curve 1). Non-saturable passive resistance would occur in the case of a partially functioning drug target, where one might find a change in the steepness of the slope of the dose-response curve. In non-saturable passive resistance, more drug would be required to obtain the same level of cell death as seen in a sensitive cell line (Figure 1B curve 2). Multiple changes in the inflection points and slopes of a dose-response curve could result from a combination of active and passive resistance mechanisms within the same cell population, and would be dependent on the concentration of the drug to which the cells were exposed. For instance, a dose-response curve may have a profile such that it started with a shoulder, followed by a steep slope with a logarithmic kill

phase, and ended with a reduction in the slope as the percentage of cells surviving approached zero. This would indicate the presence of an active resistance mechanism that eventually became saturated, followed by a range of drug concentrations to which the cell line was sensitive, ending with a passive resistance mechanism as the increasing concentration of drug exhausted its target.

1.35 The clinical benefits of an application of active/passive resistance

Currently, the most effective systemic treatment for cancer is chemotherapy. Although various approaches have been hypothesized and investigated as an alternative to chemotherapy (e.g., gene therapy, the use of oncolytic viruses, immunotherapy), these innovative approaches have yet to have a significant clinical impact (personal communication with Dr. William Mackillop, Kingston Regional Cancer Centre). Currently, the most effective treatment of cancer via systemic chemotherapy lies in the use of multiple antineoplastic agents with differing mechanisms of action (personal communication with Dr. David Stewart, Ottawa Regional Cancer Centre). Determining the nature of the dose-response relationship might thus offer some insight into the mechanisms of cell resistance that may limit chemotherapy, and suggest potential resistance modulating strategies. Additionally, it might be possible to classify different types of drug resistance into the categories of active or passive based on their mechanism of action. In a clinical application of this rationale, changes that occur in dose-response curves over several courses of treatment might also provide insight into how acquired resistance (resistance that develops and evolves over the course of treatment) differs from *de novo* resistance (resistance that is present from initiation of treatment) (Stewart *et al.*,

1996; Stewart *et al.*, 2000). Preliminary work in this field has been conducted in a clinical setting (Stewart *et al.*, 2000), where *de novo* resistance of non-small cell lung cancer to cisplatin (CP) and gemcitabine appears to be mainly due to saturable passive resistance. Conversely, resistance to vinorelbine and the taxanes appears to be mainly due to non-saturable passive resistance mechanisms. Hence, resistance modulating agents (which, as a rule, are directed against active resistance mechanisms) would not be expected to be beneficial in the treatment of non-small cell lung cancer with these agents.

For agents limited by saturable passive resistance, the optimal strategy would be to define the lowest possible effective dose and to use this low, relatively non-toxic dose in combination with other agents possessing differing mechanisms of action (Stewart *et al.*, 2000). Altering the drug schedule of administration such that it is given frequently, over a prolonged time period, could also prove useful against saturable passive resistance. For non-saturable passive resistance, one could give the highest dose of drug that could be used safely. Using drug analogs with differing physicochemical characteristics could also be helpful, as might manoeuvres to alter the tumour milieu (Stewart *et al.*, 2000). Alterations of drug administration schedule would not be expected to be of value in non-saturable passive resistance, unless such alterations permitted one to deliver a higher dose of drug. For active resistance, administration of resistance modulating agents could be of value, as could the use of the highest achievable doses of a drug, as well as rapid drug administration (Stewart *et al.*, 2000).

Figure 1: Hypothetical models for Active (A) and Passive (B) resistance. A) Active resistance (solid line) differs from the drug-sensitive cell population (dashed line) in that a shoulder appears at low doses (arrowhead). B) In the case of passive resistance, saturation of a target would result in a terminal plateau (curve 1), and a partially functioning target would result in a change in the slope of the dose-response curve (curve 2).

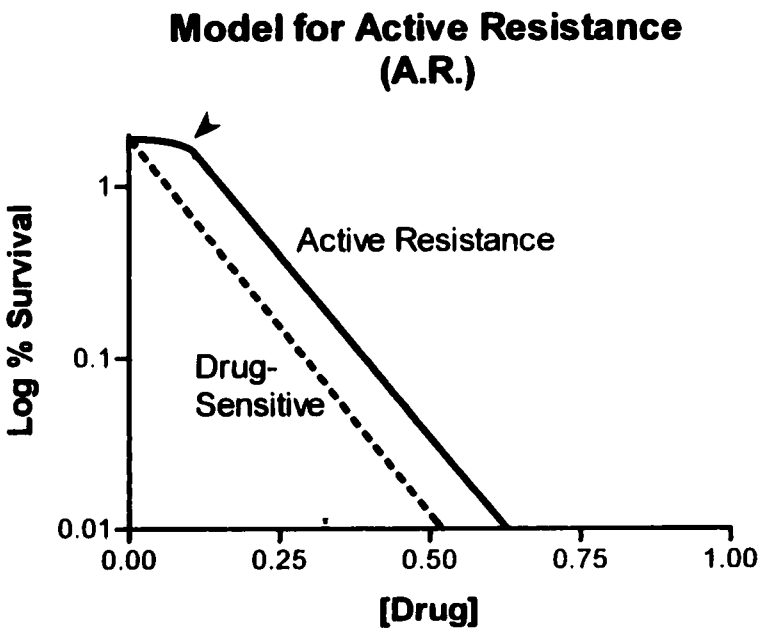
Model for Active Resistance
(A.R.)
Log % Survival
1
0.1
0.01
Active Resistance
Drug-
Sensitive
0.00
0.25
0.50
0.75
1.00
[Drug]

A

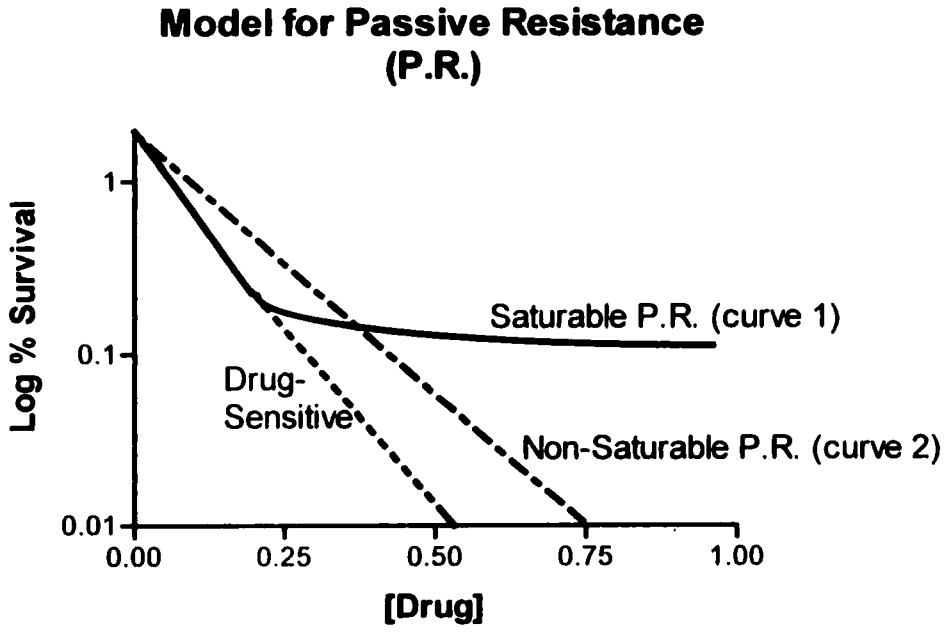
Model for Passive Resistance
(P.R.)
Log % Survival
1
0.1
0.01
Saturable P.R. (curve 1)
Drug-
Sensitive
Non-Saturable P.R. (curve 2)
0.00
0.25
0.50
0.75
1.00
[Drug]

B

1.4 Hypothesis Statement

We wish to test the hypothesis that a relationship exists between the shape of the dose-response curve and mechanisms of drug resistance. Cancers may, however, have several concurrent resistance mechanisms that could obscure the influence of any one resistance mechanism on the dose-response relationship (Redmond *et al.*, 1991; Volm *et al.*, 1998). It is therefore important to isolate one resistance mechanism found in a cancer cell, and to investigate its effect(s) on the dose-response curve.

1.5 Choosing a resistance mechanism and cytotoxic agent as a model for active/passive drug resistance

To study the concept of active and passive chemotherapeutic drug resistance, it is necessary to choose a reliable model with which to test our hypothesis. The major issue that centres around the use of a particular model is that many cancer cells possess more than one resistance mechanism that comes into play at a particular dose level. Hence, one must set up a practical system with which the effects of a single resistance mechanism can be tested. Furthermore, one must also choose a cytotoxic agent to which the model can be reliably applied. For our purposes, we have selected resistance mechanisms which would facilitate an investigation into the increased active or passive resistance to a common chemotherapeutic drug, cisplatin (CP), as that agent is one of the most efficacious against many different kinds of cancers (Beck & Dalton, 1997). The resistance mechanisms that we have chosen are the expression of wild-type p53 in a p53 deficient cell line, Saos-2, for the passive resistance model, and the transfection of γ-glutamylcysteine synthetase (γ-GCS - the rate limiting enzyme in the production of

glutathione) as a model for active resistance, introduced into a small cell lung cancer cell line (SBC-3). Both of these cell systems have been well investigated and characterized (Kurokawa *et al.*, 1995; Okaichi *et al.*, 1998; Wang *et al.*, 1998), and provide an ideal tool with which to test our hypothesis. What follows is a review of the current literature relevant to these mechanisms and our hypothesis.

1.6 Background on p53

p53 is one of the most extensively studied proteins in cancer research (reviewed in Sheikh & Fòrnace, 2000). A nuclear protein, p53 was originally considered to be an oncogene because mutated p53 alleles could transform primary rat embryo fibroblasts in concert with an activated ras gene. Cotransfection of wild-type murine p53 was found, however, to reduce transformation efficiency by many other oncogenes. These studies, and the observed diversity of mutations in many human tumours, indicated that p53 might be a tumour suppressor (Chen *et al.*, 1990; Komiya *et al.*, 1999; Sheikh & Fòrnace, 2000). It has since been implicated in many cellular processes, but its role in growth arrest and apoptosis (programmed cell death) remains undisputed. p53 acts as a transcriptional factor and mediates its effect by modulating the expression of its downstream target genes. Tumour suppression by p53 is required to maintain a non-permissive state with respect to gene amplification (Kinsella, 1997).

The p53 gene encodes a 393 amino acid phosphoprotein tetramer (Chen *et al*, 1990; Komiya *et al.*, 1999; Chen *et al.*, 1997). It has 11 exons with 5 highly conserved domains in vertebrates, and p53 mutations occur with greater frequency in these 5 regions

(Komiya *et al.*, 1999). The protein contains an amino-terminal transactivation domain, a central DNA-binding domain, and a carboxyl-terminal oligomerization domain. The NH_2 domain has transcriptional activity, and binds to a number of different molecules to regulate cell growth. For instance, both p21 and GADD45 (downstream from p53) induce cell cycle arrest and DNA repair through PCNA-dependent DNA replication, while BAX, another p53 pathway-associated protein, acts as a promoter for p53-induced apoptosis (Komiya *et al.*, 1999; Sheikh & Fòrnace, 2000). The central domain of p53 facilitates sequence-specific DNA binding to its response elements, which are present within the regulatory regions of a number of p53-regulated genes (Sheikh & Fòrnace, 2000). Homotetramerization, which takes place at the carboxy-terminal domain, as well as post-translational modifications (including phosphorylation and acetylation), are critical in modulating the binding activity of p53 to its response elements (Sheikh & Fòrnace, 2000). Since p53 plays an important role in the ability of the cell to induce cell cycle arrest, DNA repair and apoptosis, it is thus of extreme importance that it function properly. This is particularly relevant to antineoplastic drugs such as CP, whose cytotoxic functions are contingent on the ability of the cell to go into growth arrest and apoptosis consequent to DNA damage (Andrews, 1994). Changes in p53 structure and function due to mutations might thus provide a very useful model with which to test our concept of passive resistance.

1.61 The function of p53 and how it relates to drug resistance

Wild-type p53 suppresses the expression of genes that lead to cellular proliferation, and activates suppressor genes. These actions suppress tumour growth and

also have a bystander effect on neighbouring cells (Roth & Cristiano, 1997). Intact p53 function thus leads to G1 arrest and apoptosis in the cell population. Consequently, many drugs are more effective in cells with wild-type p53 (Komiya *et al.*, 1999), and a correlation has been detected between mutant p53 expression and resistance to chemotherapy (Komiya *et al.*, 1999). Conversely, using p53 genetic suppressor elements (GSE: short gene fragments expressed as either antisense RNA or dominant negative peptides), investigators have reported an up to 8-fold increase in CP resistance in A2780 human ovarian cancer cells (Perez, 1998). GSE expression was also associated with decreased p53 protein levels and loss of p53-associated functions, including cell cycle arrest and apoptosis. The effects of p53 on the cell cycle are very complex, and it is estimated that 200-300 genes may be transcriptionally activated by p53. Since p53 can also act as a repressor, there may be many other genes that may also be repressed, and the effects of these genes could potentially offset one another (Perez, 1998). p53 is a strong transcriptional activator of the gene encoding $p21^{WAF1/CIP1}$, which is a protein that mediates cell cycle arrest, and may also protect cells from apoptosis (Perez, 1998).

p53 plays an important role in genetic stability as a consequence of its ability to prevent entry of damaged cells into the S phase of the cell cycle, thus preventing the replication of damaged DNA. Many environmental toxins, including the administration of drugs such as 5-fluorouracil (5-FU), methotrexate (MTX) and N-phosphonacetyl-L-aspartic acid (PALA) increase the levels of p53 expression via damage to DNA, leading to G_1 phase arrest or apoptosis (Kinsella, 1997; Komiya *et al.*, 1999). G_1 arrest most likely involves the activation of p21, which inhibits cyclin-cdk complexes, and in turn

inhibits the phosphorylation of the RB protein and blocks progression into the S-phase of the cell cycle (Kinsella, 1997). Other factors downstream from p53 probably play a role in this as well.

p53 also affects expression of downstream genes that regulate sensitivity to apoptosis, activating the transcription of BAX (which promotes apoptosis) and repressing the transcription of Bcl-2 (which inhibits apoptosis) (Figure 2). These molecules are part of a growing family of death-agonist and antagonist proteins that control apoptosis. The death agonist (proapototic) proteins include BAX, Bak, Bcl-Xs, Bad, Bid, Bik, Bim, Hrk and Bok (Sheikh & Fòrnace, 2000). The antagonists (or antiapototic) proteins include Bcl-2, Bcl-X_L, Bcl-w, Mcl-1 and A1/Bfl-1. Both proapototic and antiapoptotic proteins contain varying domains which are homologous to Bcl-2 (designated as BH1 to BH4), and which are important for homodimeric and heterodimeric formation. The agonist:antagonist ratio is thus known to be a critical factor in controlling apoptosis (Sheikh & Fòrnace, 2000), where a BAX:BAX homodimer tends to promote apoptosis, and Bcl-2:Bcl-2 or Bcl-X_L:Bcl-X_L homodimers act as antiapototic. Heterodimeric formation of Bcl-2 with Bcl-X_L or BAX are also common, but it is not clear as to which of these several interactions is dominant, especially since mammalian cells can express multiple members of this family (Sheikh & Fòrnace, 2000). Both wild-type and mutant p53 can also have an effect on the regulation of pro- and antiapoptotic elements. All of these factors thus have a potential role in altering drug-resistance to DNA damaging agents.

The BAX promoter contains consensus binding sequences for p53, and is regulated by the wild-type, but not the mutant, p53. Transcription of Bcl-2 is repressed by wild-type p53, and thus wild-type p53 can produce reciprocal changes in BAX and Bcl-2 transcription that favour apoptosis. Altered expression of Bcl-2, Bclx and BAX genes can thus affect CP sensitivity and has been linked to changes in a cell's apoptotic ability (Komiya *et al.*, 1999; Perez, 1998; Sheikh & Fòrnace, 2000). Reduced BAX expression has thus been observed in association with p53 mutation in a CP-resistance sub-line of the IGROC human ovarian cell line. Transfection of Bcl-2 into A2780 human ovarian cells also conferred about a threefold increase in resistance to CP. Thus apoptotic regulatory genes downstream from p53 can alter sensitivity to CP (Perez, 1998).

When comparing p53 expression and the expression of downstream genes in A2780 and resistant variants with equimolar concentrations of CP, investigators found nuclear p53 levels elevated in sensitive cell lines, although BAX mRNA remained unchanged (Perez, 1998). p53 also plays a major role in resistance to 5-FU as a DNA damage response and may act in the same way for PALA and MTX (Kinsella, 1997). Much more work needs to be conducted, however, in order to elucidate the precise mechanism of p53 as a determinant of sensitivity to CP (Perez, 1998).

Figure 2: A summary of the major pathways involved in p53-mediated apoptosis, where p53 exerts an effect on the balance of pro- and anti-apoptotic factors with respect to upregulation (▲) or downregulation (▼), leading to a cascade of events which ultimately end in cell death via proteolysis. Adapted from Sheikh & Fòrnace, 2000.

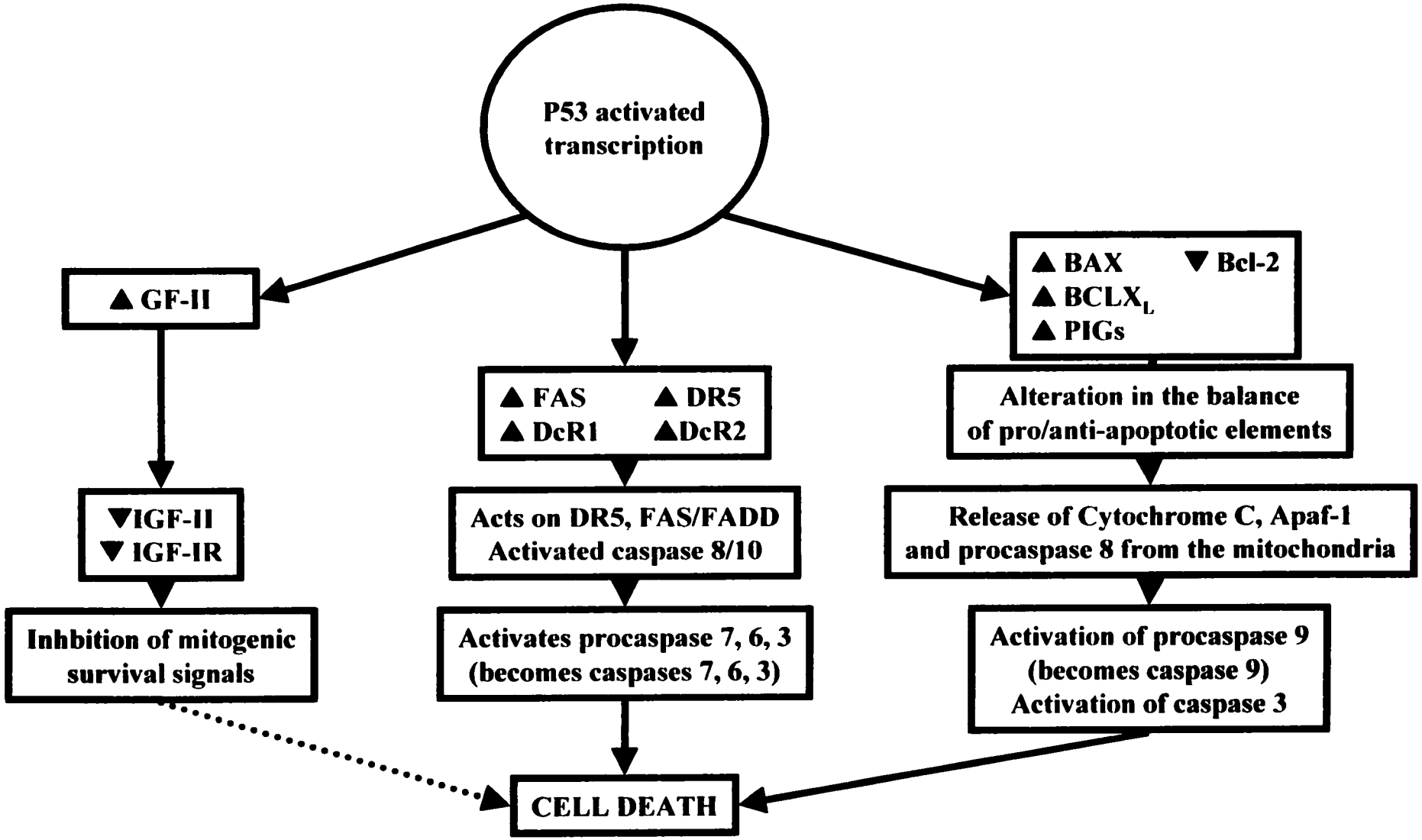
P53 activated transcription
▲ GF-II
▲ FAS ▲ DR5
▲ DcR1 ▲DcR2
▲ BAX ▼ Bcl-2
▲ BCLX$_L$
▲ PIGs
Alteration in the balance of pro/anti-apoptotic elements
▼IGF-II
▼ IGF-IR
Acts on DR5, FAS/FADD Activated caspase 8/10
Release of Cytochrome C, Apaf-1 and procaspase 8 from the mitochondria
Inhbition of mitogenic survival signals
Activates procaspase 7, 6, 3 (becomes caspases 7, 6, 3)
Activation of procaspase 9 (becomes caspase 9) Activation of caspase 3
CELL DEATH

1.62 Mutations in p53

Mutation in the p53 gene eliminates p53-dependent responses, and is one of the most common genetic changes occurring in tumour cells. p53 mutations are found in 60% of tumours overall, in 75% of colorectal malignancies, and in 50% of non-small cell lung cancer (Komiya *et al.*, 1999). The presence of a mutated or dysfunctional p53 gene permits the continued replication of damaged DNA, producing conditions that facilitate gene amplification. This is consistent with the observation that cells with no p53 protein (null mutations) amplify their DNA considerably more readily than cells containing the normal wild-type p53 gene product (Kinsella, 1997). Mutations in p53 usually occur in the open-reading frame, with 90% in exons 5-8 (including the evolutionarily conserved regions) (Komiya *et al.*, 1999), and different cancers have mutations in different codons (e.g., aa248, aa273 for lung cancer [get G to T conversions], aa175, and aa249 for colon and hepatocellular cancers [G to A conversions]). Benzo(a)pyrene, a mutagenic metabolite found in cigarettes, can also lead to G to T conversions (Komiya *et al.*, 1999). Most p53 mutations are dominant-negative, and therefore block the growth restricting function of wild-type p53 (Chen *et al.*, 1990). Mutated p53 thus functions even in the presence of wild-tvpe p53 to confer a limited growth advantage (Chen *et al.*, 1990). While p53 inactivation is extremely common in cancer cells (Schmitt & Loew, 1999), Saos-2 human osteosarcoma cells (one of the cell lines we will use in our experiments) are unique in that they completely lack a p53 gene (Chen *et al.*, 1990)

The DNA binding domain of p53 is made up of two anti-parallel β-sheets that form a scaffold and support a DNA-binding surface consisting of non-contiguous loops and helixes. This structure is subject to various mutations that can be grouped into 3 classes. Class I mutations affect residues of the DNA-binding surface (such as Arg 248, Arg 273 and disrupts protein -DNA contact points). Class II mutations affect residues crucial to the correct orientation of the DNA-binding surface (such as Arg175 & Arg249, which are involved in the connections between the scaffold and the binding surface), and may disrupt the regulation of p53 protein flexibility. Class III mutations fall within the "scaffold" and disrupt the tertiary structure of the whole DNA-binding domain. In order to detect p53-DNA mutations, one can therefore use DNA sequencing (i.e. SSCP, DGGE), or detect the altered product (which in the case of p53 would accumulate in the nuclei). Since p53 antibodies detect the C or N-terminal parts of the protein (away from the mutational hotspots), tests such as the ELISA and western blotting can also be used with confidence (Komiya *et al.*, 1999).

1.63 A review of apoptosis (programmed cell death)

Apoptosis is defined as programmed cell death (Schmidt, 1999), and has important implications for cancer therapy and many mechanisms of drug-sensitivity/resistance. The homeostasis (balance) of a cell population is maintained by proliferation and apoptosis, and apoptosis therefore regulates tumour progression/tumourigenesis (Schmitt & Loew, 1999; Zhang G, 1998). Until recently, the tumour-specific toxicity of antineoplastic agents was attributed to their effects on rapidly dividing cells. According to this model, the interaction between a compound and its

cellular target was presumed to result in massive cellular damage, disrupting crucial metabolic functions and thus causing catastrophic cell death. Consequently, efforts to understand drug resistance were largely concentrated on mutations that disrupted or prevented drug-target interactions. Based on contemporary evidence, however, the effectiveness of anticancer drugs may not simply reflect their ability to cause cellular damage, but also the cell's ability to detect and respond to this damage. Furthermore, since drugs with distinct primary targets can induce apoptosis through similar mechanisms, mutations in apoptotic programs can produce multi-drug resistance (Schmitt & Loew, 1999). *De novo* drug resistance may therefore involve selection against apoptosis during tumour development to yield multidrug-resistant cells (Schmitt & Loew, 1999).

Morphological changes during apoptosis include cell shrinkage, membrane blebbing, chromatin condensation and nuclear fragmentation (Chen *et al.*, 1999; Sheikh & Fòrnace, 2000). Programmed cell death can, however, occur without these morphological changes, long after the occurrence of death-initiating events (Schmitt & Loew, 1999). Generally, apoptotic pathways involve a sensor that induces death-inducing signal/machinery to carry out the process of cell death. This process is controlled by a series of pathways that are in turn influenced by cellular events, where the stimulus is specific to the setting (Schmitt & Loew, 1999). One receptor-linked apoptotic pathway involves "death receptors" such as Fas/CD95, TNF (tumour necrosis factor), DR3 (death receptor 3), DR4, DR5, where TNF binds to TNFR1, resulting in trimerization of the receptor and the recruitment of the signal-transducing molecule TRASS & FADD via a

conserved region of protein interaction (referred to as the death domain). This process is associated with proteolytic enzyme caspase 8, and a protease cascade that cleaves cellular targets resulting in cell death (Figure 2). Different death mechanisms associated with death receptors may depend on timing and the environment, where different branches of the apoptotic pathway may play off of each other (Schmitt & Loew, 1999). For instance, NF-kB (nuclear factor = NF; a transcription factor induced by a number of signals) was found to modulate the expression of components of death receptor complexes, enhancing apoptosis (Schmitt & Loew, 1999). Also, PI3/Akt phosphorylated death-related molecules, such as BAD, enhanced cellular survival (Schmitt & Loew, 1999).

Another apoptotic pathway, which is of particular interest to our work, is induced by DNA damage (via p53 and other pathways). In this case, DNA strand breaks are sensed by kinases (e.g. DNA-dependent protein kinase DNA-PK), and lead to the phosphorylation and activation of p53. p53 transmits the apoptotic signal by a complicated mechanism that involves, at least in part, its ability to transactivate genes such as BAX and a series of p53-inducible genes (PIGS). The subsequent step has yet to be fully understood, but it may involve changes in the mitochondrial membrane potential, and the release of cytochrome C (Schmitt & Loew, 1999). Cytosolic cytochrome C, which interacts with a multitude of proteins, complexes with ApaF1 and pro-caspase-9, leading to caspase-9 activation and the initiation of a protease cascade (Figure 2). Interruption of caspase-9 activation disrupts apoptosis in situations where p53 is required for programmed cell death (Schmitt & Loew, 1999). Apoptosis can thus be affected by

cellular context, including the tissue type and the genetic background (Schmitt & Loew, 1999).

In both apoptotic pathways, Bcl-2 affects cytochrome C release from the mitochondria and therefore modulates and/or affects ApaF2/caspase-9 inhibition (Schmitt & Loew, 1999). Terminally, the convergence of apoptotic pathways appears to activate members of the caspase family, although the relationship between deregulated caspases and changes in drug resistance has yet to be reported. Exogenous inhibition of caspases does, however, confer resistance to various drugs, and ApaF-1, caspase-2 and caspase-9 knockout mice models demonstrate this effect *in vivo* (Schmitt & Loew, 1999). Bcl-2 is therefore an important factor in the ability of p53 to trigger apoptosis, and can influence resistance to drugs whose cytotoxic effects are contingent on this pathway. Bcl-2 expression depends on the etiology of the cancer, where non-invasive, early cancers have high bcl-2 levels, and invasive/metastatic cancers have a lower level expression of bcl-2 due to a higher rate of cellular turnover (note that normal breast cells also express bcl-2). Bcl-2 is thus a useful indicator of chemotherapeutic resistance (Zhang, 1998). For instance, the level of bcl-2 is inversely related to response in the therapy of breast cancer using Tamoxifen (Zhang, 1998). In most cases, however, patients with higher detectable levels of Bcl-2 have better clinical outcomes regardless of lymph node status (Zhang, 1998), although this point is under contention. For instance, Schmitt & Loew (1999) report that overexpression of bcl-2 leads to resistance via the blocking of apoptosis, and the overexpression of bcl-2 decreases response rates in multiple myeloma. Conversely, tumours with high levels of bcl-2, considered to be resistant to chemotherapy, are

typically well differentiated and therefore have a lower histologic grade (Zhang, 1999). High bcl-2 expression also delays entry into the S-phase of the cell cycle *in vitro*, and thus slows cell cycle turnover (Zhang, 1998).

Many other mitogenic oncogenes, while forcing uncontrolled proliferation, can also enhance apoptosis (e.g., myc, E1A, E2F-1, cdc25, ras) (Schmitt & Loew, 1999). Apoptosis is facilitated by tissue hypoxia and low concentrations of growth factors, and thus environmental factors have an effect, possibly implying a fail-safe mechanism in the event of genetic mutations (Schmitt & Loew, 1999). Note that other members of the bcl family (e.g., bcl-xS, bak) promote apoptosis (Schmitt & Loew, 1999). Finally, BAX deficiencies mediate drug resistance, where its overexpression enhances radiosensitivity or sensitises cells to anti-cancer drugs, and regulation is believed to occur via the formation of dimeric complexes (Schmitt & Loew, 1999).

1.64 The clinical relevancy of alterations in p53

Although the cascade of events initiated by p53 activation are very complex and have yet to be fully mapped out, the clinical outcomes of deficiencies in p53 function have been well studied. Alterations in p53 result in a significantly poorer prognosis for patients, *de novo* or acquired resistance and relapse (Komiya *et al.*, 1999; Schmitt & Loew, 1999). p53 is thus a good marker for cancer detection and diagnosis, where the degree of (mutant) p53 accumulation is linked to an increase in the severity of dysplasia. p53 is also a good clonal marker (Komiya *et al.*, 1999), and MdM2 overexpression leads to p53 degradation and early treatment failure (Schmitt & Loew, 1999).

The function of p53 is integral in many cellular pathways that are activated by the cytotoxicity of antineoplastic agents. This protein is thus a keystone in a complex web of molecular interactions that have important consequences for the cell's ability to undergo apoptosis following exposure to anticancer drugs. Although considerable work is required in order to fully understand the various pathways that lead to cell cycle arrest and apoptosis (not to mention the complication of environmental influences on this system), it is virtually indisputable that p53 plays a major role in determining the apoptotic response of the cell to cytotoxic agents. Mutations in p53, which is a target for the action of many drugs, thus enables us to use it as a paradoxically simple and rather elegant tool for an investigation into the concept of passive resistance. Since p53 functions as a target for drug action, it would follow based on our hypothesis of drug resistance that a cell type with non-functional mutant p53 would display a profile congruent with saturable passive resistance. The use of p53 as a model for passive resistance is made even more appropriate, since considerable data has been reported on its abilities to exert an important influence at the clinical level.

1.7 Background on glutathione

In 1888, an intrepid investigator named Rey Pailhade discovered a substance that he called "hydrogénant de soufre", which later proved to be glutathione (L-γ-glutamyl-L-cysteinylglycine [GSH]). GSH is synthesized from its constituent amino acids by many prokaryotes of the eubacteriotic kingdom, as well as by virtually all eukaryotic cells (*Entamoeba histolytica* & *Giardia* being the major exceptions thus far) (Griffith &

Mulcahy, 1999). Subsequent work revealed that this substance had an antioxidant function, and thus it sparked an interest in the area of microbial antioxidant defence (Sies, 1999). Glutathione is now known to be a tripeptide (m.w. 307) that provides cells with a reducing environment, and accounts for the majority of the intracellular nonprotein sulfhydryl content of many cell types (Griffith & Mulcahy, 1999). In mammalian tissues, intracellular GSH concentrations (0.5-10 mM) exceed that of most amino acids, such as L-cysteine (which ranges from 15-500 μM) (Griffith, 1999).

The high tissue concentration and wide range of biological distribution of GSH is consistent with the many roles played by that tripeptide. GSH has many important functions in animals, including transport and storage of cysteine (Higashi *et al.*, 1977, Tateishi *et al.*, 1977), and acts as a co-factor in several enzymatic reactions (e.g. Glyoxylase I and II, as well as formaldehyde dehydrogenase) (Inoue & Kimura, 1995, Koivusalo *et al.*, 1989). It has important functions in metabolism, DNA synthesis, and the protection of cells against the toxic effects of oxygen and other compounds (Beutler *et al.*, 1999; Griffith, 1999; Lai *et al.*, 1989; Sies, 1999; Yan and Meister, 1990). Among the toxins inactivated by GSH are the reactive oxygen species (e.g. hydroxyl radical and hydroperoxides), reactive nitrogen species (e.g. peroxynitrite and N_2O_2), and reactive electrophiles (e.g. activated metabolites formed by the cytochrome P-450 system and bifunctional DNA alkylating agents used in cancer chemotherapy, such as CP) (Griffith & Mulcahy, 1999). Mammalian cells contain between 1 and 10 mM glutathione located in sub-cellular pools (Soltanninassab *et al.*, 2000), with the majority located in the cytosol and nucleus in reduced form (GSH), with only a small amount oxidized to glutathione

disulphide (GSSG) (Griffith, 2000). Cellular GSH levels reflect a steady state balance between synthesis and loss (Griffith, 1999), although once synthesized, GSH can undergo transport across the plasma membrane, to become part of a complicated inter-organ network (Sies, 1999). The finding that elevated GSH levels contribute to the resistance of many tumours to radiation therapy, chemotherapeutic DNA cross-linking agents and redox cycling drugs, has stimulated interest in the pharmacological regulation of GSH as a therapeutic modality (Ahmad *et al.*, 1987; Arrick & Nathan, 1984; Colvin *et al.*, 1993; Griffith & Friedman, 1991; Meister & Griffith, 1979; O'Brien & Tew, 1996; O'Dwyer *et al.* 1995; Schröder *et al.*, 1996).

1.71 The synthesis and fate of glutathione

The synthesis of glutathione occurs in two steps. In the first reaction (i), catalyzed by γ-GCS, a peptide bond is formed between the γ-carboxyl group of glutamic acid and the amino group of cysteine. Next, glutathione synthetase catalyses the formation of a peptide bond between the carboxyl group of the cysteine of γ-glutamylcysteine and glycine (ii). In each of these reactions, a molecule of ATP is dephosphorylated to ADP (Beutler *et al.*, 1999; Griffith, 1999; Yan and Meister, 1990).

i. L-Glutamate + L-cysteine + MgATP ⇔ L-γ-glutamyl-L-cysteine + MgADP + P_i

ii. L-γ-glutamyl-L-cysteine + glycine + MgATP ⇔ GSH + MgADP + P_i

In mammals, these reactions take place in the cytosol, where the rate of GSH synthesis is controlled by the amount of γ-GCS present, by the availability of L-cysteine,

and by feedback inhibition of γ-GCS exerted by high concentrations of GSH. GSH synthetase does not appear to have a regulatory role, where γ-glutamylcysteine (once synthesised) is rapidly converted to GSH (Griffith & Mulcahy, 1991). Glutathione is not degraded in cells, rather it is constantly secreted and then degraded extracellularly by γ-glutamyl transpeptidase. Additional extracellular and intracellular enzymes degrade the resultant γ-glutamylamino acids and cysteinylglycine into constituent amino acids that can be used for various purposes, including the resynthesis of GSH (Griffith & Mulcahy, 1991) (Figure 3A).

The major fates of glutathione are hydrolytic cleavage and disulfide formation, as well as thioether and thiolester formation (Sies, 1999). A group of glutathione-S-tranferases (GSTs) generate a large set of thioethers, termed glutathione-S-conjugates that are committed to detoxification and elimination (Sies, 1999). GSH thus has a function in Phase II detoxification, leading to sequential modification, biliary excretion, and inter-organ transport for final renal excretion (Soltanninassab *et al.*, 2000; Sies, 1999).

Figure 3. Simplified pathways of GSH synthesis (A) and fate (with respect to chemoprotection) (B). A) GSH is synthesized from its constitutive amino acids in the cytosol, and is consecutively excreted from the cell where is it degraded by γ-glutamyl transpeptidase. CysH-gly is broken down by dipeptidases into cysteine, and then transported into the cell. Glu is transported into the cell once formed, and these amino acids re-enter the GSH synthesis cycle. B) Conjugates (designated as X) can bind enzymatically or non-enzymatically to GSH, and are effluxed via GS-X active transporters. They are then sequestered in the mercapturic acid pathway for eventual excretion into the urine. Cysteine and Glutamate are typically recovered for re-entry into the cycle of GSH synthesis. Adapted from Griffith, 1999, and Zhang *et al.*, 1998.

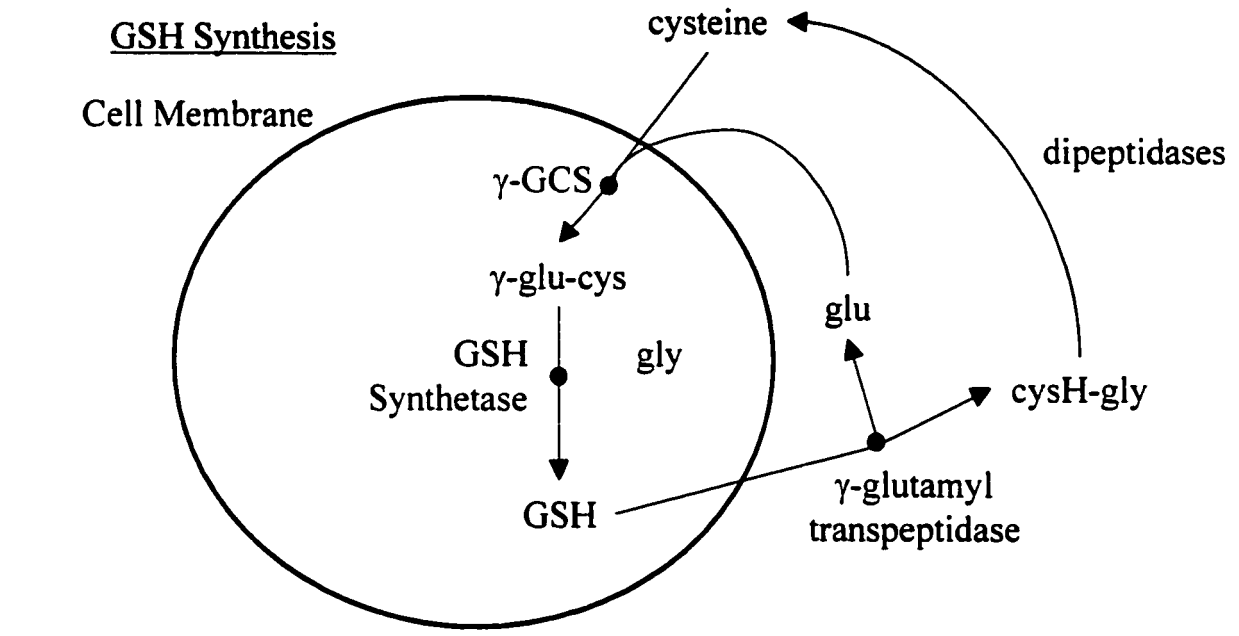
GSH Synthesis
cysteine
Cell Membrane
dipeptidases
γ-GCS
γ-glu-cys
glu
GSH
Synthetase
gly
cysH-gly
γ-glutamyl
transpeptidase
GSH

A)

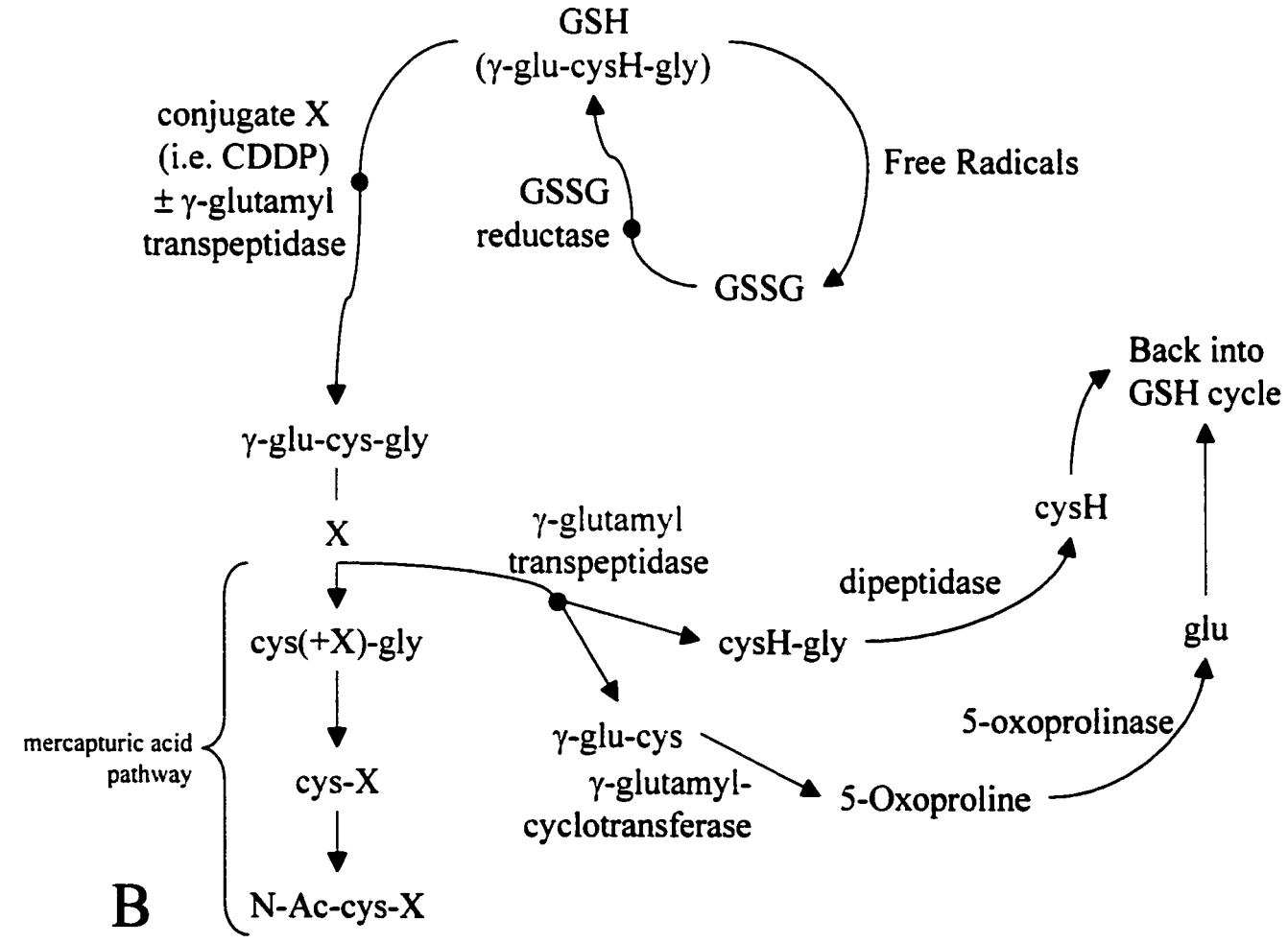
Fate of GSH (chemoprotection)
GSH
(γ-glu-cysH-gly)
conjugate X
(i.e. CDDP)
± γ-glutamyl
transpeptidase
GSSG
reductase
Free Radicals
GSSG
Back into
GSH cycle
γ-glu-cys-gly
X
γ-glutamyl
transpeptidase
cysH
dipeptidase
cys(+X)-gly
cysH-gly
glu
5-oxoprolinase
mercapturic acid
pathway
γ-glu-cys
γ-glutamyl-
cyclotransferase
5-Oxoproline
cys-X
N-Ac-cys-X
B

1.72 The function of glutathione (and drug resistance)

The protective functions of GSH occur both enzymatically and nonenzymatically, where GSH reacts directly with toxic species (e.g. hydroxyl radical and peroxynitrite, and requires enzymatic catalysis to detoxify other less reactive species (e.g., GSH peroxidases mediate detoxification of hydroperoxides). Adduct formation between GSH and reactive electrophiles such as activated phosphoramide mustard occur spontaneously and with GSH S-transferase catalysis (Griffith & Mulcahy, 1999). Glutathione also serves to maintain other low molecular weight antioxidants (such as ascorbate (vitamin C) and α-tocopherol (vitamin E) in their biologically active form (Meister, 1994). All of these protective reactions depend on the cysteine residues of GSH, and the GSH thiol is notable for its reactivity with toxic species, as well as its resistance to auto-oxidation (Griffith & Mulcahy, 1999). GSH reacts quickly and nonenzymatically with hydroxyl radicals, the cytotoxic fenton product, N_2O_3, and peroxynitrite, which are cytotoxic products formed by the reaction of nitric oxide with O_2 and superoxide, respectively. GSH also participates in the reductive detoxification of hydrogen peroxide and lipid peroxides (Griffith, 1999). Furthermore, GSH has a role in signal transduction, gene expression, apoptosis, and there are links between the thiol redox state, glutathione-protein interactions, and cell proliferation. Protein glutathionylation may thus have a role in such processes (Hall, 1999; Sies, 1999).

All of the protective functions of GSH result in its stoichiometric consumption and conversion to nonprotectant products. For example, GSH reacts with most

electrophiles to form a stable thiol adduct (typically a sulfide) which is then metabolized to mercapturic acid and excreted in the urine (Figure 3B) (Griffith & Mulcahy, 1999). Although the glutamyl and glycyl residues of GSH are salvaged, the cysteinyl moiety is excreted as part of the mercapturic acid (Figure 3B), and must be restored by *de novo* synthesis. Consequently, low levels of cysteine, or the reduced capacity to synthesize GSH consumed via the detoxification of electrophiles can compromise cell survival. The GSH-mediated protection from reactive oxygen species, however, results in the oxidation of GSH to GSSG. In general, GSSG does not accumulate, but is rapidly reduced back to GSH by NADPH in a reaction catalyzed by GSSG reductase (Figure 3B). *De novo* synthesis of GSH is therefore not required in this pathway. Even if the capacity of GSSG reductase or the supply of NADPH was exceeded, a fraction of the GSSG formed may be preferentially excreted by the cell but, even in this situation, all the constituent amino acids would be eventually recovered after extracellular degradation of GSSG (Griffith & Mulcahy, 1999). At physiological levels of NADPH and $NADP^+$, the GSSG reductase reaction is driven strongly in favour of GSH and the intracellular ratio of GSH:GSSG is typically close to 99:1, maximizing the antioxidant capacity of the GSH pool (Gilbert, 1990; Zeigler, 1985).

At biological concentrations of 0.5-10 mM, GSH conjugates with DNA-binding drugs, such as the alkylating agents melphalan, CP, chlorambucil, mechlorethamine, cyclophosphamide, phosphoramine, ifosfamide, and many other compounds (Zhang, 1998). Conjugated drugs acquire a negative charge by conjugation to GSH via sulphoxidation or glucuronidation. Glutathione S-conjugates and glucuronides are then

effluxed (Keppler, 1997) by a GS-X pump, which plays a major role in the export of anti-cancer drugs from tumour cells (Kurokawa *et al.*, 1995; Zhang, 1998). The elevation of thiols, including GSH, results in radioprotection and a decrease in sensitivity to many anticancer drugs, including cisplatin (Lai *et al.*, 1989). Consequently, cell lines resistant to electrophilic stress have been found to have high levels of intracellular GSH, as well as increased levels of γ-GCS (Soltanninassab *et al.*, 2000; Ogretemen *et al.*, 1998; Tew *et al.*, 1996). Conversely, abnormally low levels of glutathione are detected in cells with deficiencies in γ-GCS, although this deficiency is rare (Beutler *et al.*, 1999).

A linear correlation between GSH levels and CP resistance has been reported in human renal, bladder, ovarian cell lines and biopsies (Perez, 1998). Elevated GSH content leads to CP resistance, where GSH-Pt conjugates correspond to 60% of intracellular Pt content in murine Leukemia L1210 cells. Inhibition of protein synthesis consequently leads to an increase in CP toxicity (Zhang, 1998). GSH is thus a good model for biomodulation because it potentially affects CP sensitivity in a number of different ways (i.e. binding CP in cytoplasm, monofunctionally binding to DNA and active transport of the GSH-Pt complex [efflux]) Depletion of GSH by buthionine sulfoximine (BSO) inhibits DNA repair, and GSH may modulate the active site cysteine residues of HMG-1 and HMG-2 proteins, (which are necessary in order to recognise DNA-induced damage). GSH may also modulate transcription factors that potentially affect DNA repair and apoptosis, such as c-fos and c-jun (Hall, 1999; Perez, 1998), and therefore may exert a significant role in drug resistance.

The drug resistance profile of cells expressing high levels of GSH, as reported in the literature, makes it an excellent candidate as a model for the study of active resistance. The synthesis of GSH is thus of particular interest in regards to active resistance, as increased synthesis should result in a decreased chemotherapeutic effect of antineoplastic drugs. A review of the role of γ-GCS, which is key in the production of GSH, provides additional support in the use of this system as a model for active resistance.

1.73 An introduction to γ-glutamylcysteine synthetase (γ-GCS)

Gamma-glutamylcysteine synthetase (γ-GCS) is the rate limiting enzyme in GSH synthesis. γ-GCS consists of a heavy (M_r ~73000) and a light subunit (M_r ~ 31000), where the heavy subunit has catalytic properties and contains all of the substrate binding sites. The light subunit exerts a regulatory function, modulating the affinity of the heavy subunit for the substrate and various inhibitors. The light subunit is not enzymatically active, nor does it alter the catalytic properties or stability of the heavy subunit (Yan and Meister, 1990). It has been suggested that under normal conditions the light subunit of γ-GCS is stabilized by the heavy subunit, and in its absence is proteolysed (Beutler *et al.*, 1999; Griffith, 1999; Griffith & Mulcahy, 1999; Soltanninassab *et al.*, 2000). Although the heavy subunit maintains a catalytic capacity, studies in the elevation of GSH levels after transfection of both the heavy and light subunits in differing ratios demonstrate that the highest levels of GSH are produced when both subunits are present in a 1:1 ratio (Mulcahy *et al.*, 1995). Thus, it is possible that optimal rates of GSH synthesis are compromised by the absence of the lighter subunit.

1.74 The regulation and overexpression of γ-GCS

γ-GCS activity is controlled by feedback inhibition by GSH, where GSH acts as a non-allosteric feedback inhibitor competitive with L-glutamate (Ki^{GSH} = 2.3 mM), and is dependent on the cysteinyl thiol group, where the glutamyl residue occupies the binding site (Griffith, 1999; Soltanninassab *et al.*, 2000; Yan and Meister, 1990). Mammalian γ-GCS is an enzyme that is activated by the formation of reversible disulfide bonds, and there appears to be at least 2 pairs of disulfide bonds that are required for optimal enzyme activity. One of these bonds, linking the heavy and light chain, can be reduced at high GSH concentrations. Depletion of GSH promotes the formation of the disulfide bonds and promotes optimal enzyme activity though changes in enzyme conformation (Soltanninassab *et al.*, 2000).

Overexpression of γ-GCS in vivo has been linked to increased GSH levels and increased drug resistance, while deficiencies in γ-GCS are linked to serious disorders such as hemolytic anemia (Beutler *et al.*, 1999; Soltanninassab *et al.*, 2000; Zhang, 1998). γ-GCS overexpression also confers drug resistance by activating the GS-X pump (Kurokawa *et al.*, 1995; Zhang, 1998). As GSH is a ubiquitous protein, γ-GCS is present in many cell lines, and a strong correlation between γ-GCS levels and resistance to alkylating agents, such as cisplatin, has been reported (Tew *et al.*, 1996). Furthermore, one of the earliest and most common biochemical changes in preclinical models of alkylating agent resistance is an elevation of intracellular levels of GSH (Griffith & Friedman, 1991; Colvin *et al.*, 1993; O'Dwyer *et al.*, 1995, O'Brien & Tew, 1996;

Schröder *et al.*, 1996). In contrast, none of the other glutathione-related enzymes have patterns of expression that resulted in an obvious correlation to the sensitivity or resistance to alkylating drugs, including platinum agents (Tew *et al.*, 1996). Of all the GSH-related enzymes, γ-GCS was thus found to be an important determinant of cellular response to alkylating agents (Tew *et al.*, 1996). The linkage between GSH and drug resistance is further strengthened by studies indicating that pharmacological depletion of intracellular levels of GSH results in increased drug sensitivity (Griffith & Friedman, 1991; Colvin *et al.*, 1993; O'Dwyer *et al.*, 1995, O'Brien & Tew, 1996; Schröder *et al.*, 1996), and that transfection of both γ-GCS subunit cDNA results in increased γ-GCS activity, higher intracellular levels of GSH, and resistance to melphalan (Mulcahy *et al.*, 1995).

The mechanisms by which GSH protects cancer cells from toxic insult are presumably the same as those applicable to normal cells. Consistent with this view, elevated levels of GSH are frequently seen in tumours resistant to various chemotherapeutic agents. In addition, GSH has a functional role with certain DNA repair enzymes (Colvin *et al.*, 1991; O'Dwyer *et al.*, 1995; O'Brien & Tew, 1996), and its elevation can thus facilitate the repair of drug-induced DNA lesions (Griffith & Mulcahy, 1999). While high levels of γ-GCS can confer resistance to therapy (Griffith, 1999), depletion of GSH by buthionine sulfoximine (BSO), a potent inhibitor of γ-GCS, renders both normal and cancer cells more sensitive to radiotherapy (Lai *et al.*, 1989; Sies, 1999). BSO is considered to be an irreversible inhibitor of γ-GCS because its phosphorylated product, L-Buthionine-S-sulfoximine phosphate, binds covalently to the γ-GCS active

site (Griffith, 1999; Meister, 1995). Even a 20% inhibition of γ-GCS can have a biologically significant effect on GSH levels (Griffith, 1999). GSH-mediated resistance to a drug may thus be a function of the cells ability to regulate the translation and transcription of detoxifying enzymes (Tew *et al.*, 1996). More recently, new active transporters capable of recognizing GSH-drug conjugates and transporting them out of the cells have been identified, providing another mechanism for elevated GSH-related resistance (Griffith & Mulcahy, 1999).

The activity of γ-GCS, and its association with increased levels of GSH thus make it an ideal candidate for experimental manipulation in our study of active resistance. Additional copies of the full-length coding region of γ-GCS would presumably lead to increased levels of GSH, and an increased resistance of the cell to CP.

2. MATERIALS AND METHODS

2.1 Description of the cell lines and the transfectants

Human small-cell lung cancer (SBC-3) and human osteosarcoma (Saos-2) cells were used throughout these experiments. SBC-3 cells were transfected with the human gene encoding γ-glutamylcysteine synthetase (termed SBC-3/GCS) and Saos-2 cells (which in their natural state have no p53) were transfected with the human gene encoding p53 (termed Saos-2/p53). These transfectants were used for the comparison of active and passive resistance mechanisms, respectively, and were established previously by other investigators. Consequently, these cells have been well characterized in regards to their acquired properties (Kurokawa *et al.*, 1995; Okaichi *et al.*, 1998; Wang *et al.*, 1998).

2.11 The transfection of γ-GCS into SBC-3 cells

Briefly, the full-length coding region of γ-GCS was obtained via PCR amplification, where the original plasmid (pYEUra3) was obtained from a human thymus cDNA library. The 2.0-kb PCR product was subcloned into the (eukaryotic) expression vector pCR3, which contains the bacterial neomycin phosphotransferase (neo) gene, and confers resistance to the antibiotic geneticin (G418). This construct was transfected into SBC-3 cells using the Fugene™6 Transfection Reagent, supplied by Boehringer Mannheim (Quebec, Canada), and transfected cells were selected using 1 mg/ml G418. Selective pressures to ensure that the transfected population remained homogenous for the gene of interest were maintained throughout all experiments (i.e. the addition of G418

to the growth medium), except in the case of assays involving cisplatin exposure, in order to address the slight possibility that G418 and cisplatin might would interact in a sub- or supra-additive fashion.

2.12 The transfection of wild-type p53 into Saos-2 cells

In the case of Saos-2 cells, a LacSwitch inducible mammalian expression system, supplied by Stratagene (La Jolla, USA) was used. The expression plasmid was pOPI3(CAT), where the CAT gene was replaced by wild-type p53 at the Not I restriction enzyme sites. Transfection was carried out using the calcium phosphate precipitation method, as described by Chen & Okayama (1987), and transfectants which contained the double vector system were selected using 100 μg/ml of the antibiotic hygromycin, as well as 400 μg/ml G418. By using this system, high levels of p53 expression could be obtained in the transfectants (Saos-2/p53) following 24-hour exposure to 5 mM Isopropylthio-β-D-galactoside (IPTG). In the absence of IPTG, p53 gene expression was largely suppressed. Selective pressures to ensure that the transfected population remained homogenous for the gene of interest were maintained throughout all experiments (i.e. the addition of both hygomycin and G418 to the growth medium), except in the case of assays involving cisplatin exposure, in order to address the slight possibility that one of both of the drugs might interact with cisplatin in a sub- or supra-additive fashion.

2.2 Cell culture conditions and growth characterization

The cells were grown in 25 or 75 cm^2 tissue culture flasks in a sterile incubator set at 37°C with a humidified atmosphere of 5% CO_2. The cells were maintained in logarithmic growth in "complete" culture medium consisting of RPMI 1640, containing 10% heat-inactivated fetal calf serum for SBC-3 cells, and DMEM containing 10% heat-inactivated fetal calf serum for Saos-2 cells.

For the assay of SBC-3/Saos-2 growth curves (as described in Freshney, 1994), 10^4 cells were seeded in 25 cm^2 culture flasks with 5 ml RPMI 1640/DMEM media, respectively. Three flasks were trypsinized each day and the concentration of cells/flask was determined using a hemocytometer subsequent to staining any dead cells with trypan blue. Concurrently, (after the sixth day) another set of flasks were trypsinized which had the cell culture media changed after 6 days, and these results were compared to cells which had not undergone a change in media. The doubling time was estimated via linear regression of a fitted line through the exponential growth phase using Graphpad Prism (version 3.02).

2.3 The presence of p53 in Saos-2/p53 cells, and γ-GCS in SBC-3 cells

2.31 Extraction of proteins from cells

Saos-2 cells, SBC-3 cells and their transfectants were analyzed for the presence and relative quantities of p53 or γ-GCS, respectively. The cell culture medium was removed, and cells were rinsed twice in sterile phosphate-buffered saline solution (PBS).

Cells were trypsinized, collected in medium, and centrifuged for 10 minutes at 1500 rpm. The pellet was resuspended in PBS, and centrifuged at 1500 rpm for 10 minutes. The resultant pellet was resuspended in RIPA lysis buffer (1% NP40, 0.5% Deoxycholate, 0.1% SDS in PBS, with inhibitors PMSP [10 µg/ml], NaOrthovanadate [10 µl/ml], and Aprotinin [30 µg/ml]), and kept on ice for 10 minutes. During this time, the samples were run through a 26 gauge needle to shear DNA and to ensure a complete lysis of the sample. The solutions were then centrifuged at 1500 rpm for 20 minutes at 4°C, and the supernatant was transferred to pre-chilled microfuge tubes for storage at -85°C.

Protein concentration was determined using the $^{D}_{C}$ Protein Assay kit, supplied by BioRad Laboratories (California, USA), as outlined in the instructions as supplied, to permit equal loading of the SDS-PAGE gel wells.

2.32 Protein separation using SDS-polyacrylamide gel electrophoresis (PAGE)

A 12% acrylamide separating gel (5 ml Acrylamide/Bisacrylamide (25%:0.25%), 2 ml Tris/Glycine [0.5M:1.5M], 1 ml 50% Glycerol, 0.4 ml 10% SDS, 3 ml DDW, 150 µ 10% Ammonium persulphate, 10 µl TEMED) was cast and allowed to polymerize completely (approximately 30 minutes) while overlaid with isopropyl alcohol. Once polymerization was complete, the isopropyl alcohol was carefully removed, and a 4% acrylamide loading gel was cast (670 µl Acrylamide/Bisacrylamide (30%:2.7%), 1.25 ml 0.5M Tris-HCl (pH 6.8), 50 µl 10% (w/v) SDS, 2.5 ml DDW, 25 µl 10% Ammonium persulphate and 2 µl TEMED). A 10-well comb was inserted into the stacking gel, which was allowed to completely polymerize (approximately 15 minutes). Cell extracts were

permitted to thaw completely, and were thoroughly mixed prior to use. Cell extracts were mixed with loading buffer (4 ml DDW, 1 ml 0.5M Tris-HCl (pH 6.8), 800 µl Glycerol (1.257 g/ml), 1.6 ml 10% (w/v) SDS, 400 µl 2-ß-mercaptoethanol, 200 µl 0.1% (w/v) bromophenol blue) in a 1:1 ratio, and loaded into the wells to achieve a total protein content of 25 µg/ml in each well. A pre-made broad range protein standard (6.9-205 kDa), supplied by BioRad Laboratories (California, USA) was loaded into one well to aid in the identification of the p53/γ-GCS band at the appropriate molecular weight. The running buffer consisted of 120.8g Tris base, 225.6g Glycine, 4g SDS made to 4L with DDW and was stored at room temperature. The gel was run at constant voltage of 100V, and cooled via convection with cold water, until completion.

2.33 Electrotransfer of separated proteins

Following SDS-PAGE, the gel was equilibrated for 10 minutes in electrotransfer buffer (2.9 g Tris, 5.8g Glycine, 200 ml Methanol, made to 1L with DDW) along with Whatman #1 filter paper, nylon transfer membrane (pre-soaked in methanol), and fibre pads. The gel cassette was assembled and the electrotransfer was permitted to run at a constant voltage of 1 hour at 400 mA (on ice, at 4°C). The presence of protein on the membrane was confirmed by staining with Ponceau Red. The membrane was then de-stained in Tris-buffered PBS (6.08 g Tris base, 8.76g NaCl; pH 7.5 in 1L DDW) with 0.1% Tween (TBS-T) in preparation for the Western Blot.

2.34 Western blotting

In order to reduce the background caused by non-specific binding of immunological reagents to the transfer membrane, the membrane was incubated in nonfat dried milk (Carnation powdered, diluted in PBS at 5% w/v) overnight at 4°C. Incubation with a primary mouse monoclonal antibody against p53 (1.5 μg/ml) or a rabbit polycloncal γ-GCS_h (1/8000 dilution) in 5% w/v milk followed for one hour at room temperature. The membranes were then rinsed in TBS-T for 3X15 minutes. The membranes were subsequently incubated at room temperature for 35 minutes with a horseradish peroxidase-conjugated secondary rabbit (goat anti-mouse secondary antibody [1/5000], or goat anti-rabbit [1/8000]). The membranes were rinsed in TBS-T for 3X15 minutes, and carefully blotted in preparation for detection via enhanced chemiluminescence.

2.35 Detection of proteins using enhanced chemiluminescence

This assay was performed as outlined in the instructions found for enhanced chemiluminescence detection provided in an ECL kit supplied by Amersham Pharmacia Biotech UK (England). Briefly, the transfer membranes were immersed in a detection reagent (1/1 ratio of solutions A and B) for 5 minutes. Extra reagent was blotted clear of the membrane, which was then sandwiched between clear plastic film. Working in a dark room, the plastic-covered membrane was placed protein side up and placed in an x-ray film cassette, and overlaid with enhanced chemiluminescence (ECL) hyperfilm. The cassette was closed to allow an initial film exposure of approximately 2 minutes. Once

two minutes had passed, the x-ray cassette was opened, and the film was placed into an automatic developer/fixer. Subsequent exposures were made as needed to obtain optimal visualization of the bands of interest. Varying exposure times were based on the quality of exposure obtained in the original two minutes.

Following exposure of the x-ray film, the relative differences between signal intensity was determined. The blots were scanned electronically, and the resultant images were analyzed using ImageQuant (version 4.2a Build 13). The relative intensities were then normalized to a baseline value of 100%. In the case of Saos-2 cells, the baseline chosen was the expression of p53 in the non-induced Saos-2 cells (Saos-2/p53). In the case of the SBC-3 cell line, the level of γ-GCS expression in the parent cell line (SBC-3) was chosen as the baseline. These normalized values were then compared via an unpaired t-test, carried out by GraphPad Prism version 3.02 for Windows (GraphPad Software, San Diego California USA, www.graphpad.com).

2.4 Flow cytometry

In order to characterize the DNA content and cell cycle distribution of the cell lines used in our assays, we conducted a flow cytometric analysis. We also exposed the cell populations to 1 hour of cisplatin in order to observe the effects of the drug on the cell cycle ditribution of the parent and the transfectant cell lines. Saos-2 parent and transfectant cells were thus exposed to 4 μg/ml, since this corresponded to the LD_{20} the clongenic dose-response curve. SBC-3 cells were exposed to 0.8 μg/ml of cisplatin (for 1

hour), since this corresponded to the LD_{20} of that cell line. The LD_{20} was chosen arbitrarily as a drug concentration that would be sufficient to obtain a significant cytotoxic reponse to cisplatin wihout resulting in complete colony death. of Saos-2 cells, SBC-3 cells and their transfectants, $2x10^6$ cells were harvested via trypsinization and suspended in 2 ml PBS. The cell suspensions were added dropwise into ice-cold 70% ethanol. The ethanol solution was vortexed during addition of the cells to prevent clumping. Cells fixed in ethanol were stored at -20°C until analysis via flow cytometry. On the day of the assay, the cells were centrifuged at 1500 rpm for 10 minutes, and the ethanol was aspirated. The pellet was rinsed in PBS, recollected, and resuspended in 1 ml of PBS containing 100 µl of RNAase (100 µg/ml) for incubation (1 hour at 37°C). Following this incubation, 900µl of 5 µg/ml propidium iodide were added to the cell suspension, and were incubated on ice for 30 minutes. Each sample was passed gently through a 22 gauge needle to ensure that the suspension was well separated, after which their DNA content was determined via flow cytometry (Ormerod *et al.*, 1994-b). The resulting histograms were analysed using the Mutlicycle AV program (version 3.11).

2.5 Assay to measure reduced glutathione

SBC-3 and SBC-3/GCS cells were maintained in culture and collected as described above. In order to measure the effects of buthionine sulfoximine (BSO) inhibition on GCS activity, SBC-3 and SBC-3/GCS cells were also exposed to 10 or 100 µM BSO for 24 hours prior to harvesting the cells for GSH quantification. Non-confluent treatment and control flasks were prepared, and the treatment flasks were exposed to cisplatin (0.8 µg/ml) for one hour. Following drug exposure, treatment and control flasks

were rinsed twice with PBS, trypsinized, and suspended in culture medium. Samples were transferred to 15 ml centrifuge tubes, and were centrifuged at 1500 rpm for 10 minutes (at 4°C). The resultant pellet was resuspended in ice-cold PBS as a final washing stage, transferred to a 1.5 ml Eppendorf microfuge tube and spun down. The PBS was aspirated, and the cell pellet was rapidly resuspended in 100 µl DDW and 100 µl 2N Perchloric acid. Samples were vortexed vigorously to mix, held at 0°C for 15 minutes, and centrifuged at high speed for 1 minute. 150 µl of the supernatant were transferred to a fresh Eppendorf tube, and 150 µl of 1N KOH were added to neutralize the acid solution. The original tubes, whose pellet contained the protein precipitate of each sample, were kept for subsequent protein quantification. Eppendorf tubes containing the supernatant and KOH were vortexed vigorously and held at 0°C for 15 minutes. The samples were centrifuged at high speed for 1 minute and 200 µl of the supernatant were diluted in 2.3 ml of buffer A (0.1M K_2HPO_4/1mM EDTA pH 8.0). GSH standards (0-600 pmol) were prepared from a freshly prepared solution of 1mM GSH. 25 µl of 1mg/ml o-Phthaldehyde were added to each tube, which were incubated in the dark for 20 minutes at room temperature.

Following the incubation, GSH levels of samples and standards were determined by fluorescence spectrophotometry at an excitatory wavelength of 350λ and an emission wavelength of 420 λ, using a LS-5 Fluorescence Spectrophotometer (Perkin Elmer, USA). GSH absorbencies were determined via linear regression analysis of the standard curves using GraphPad Prism version 3.02 for Windows (GraphPad Software, San Diego California USA, www.graphpad.com).

The total protein of each sample, following its precipitation during exposure to perchloric acid as described above, was determined using a fluorescamine assay. Briefly, the remaining supernatant in each tube was aspirated, and 200 µl of ice-cold PBS were added. The pellet was resuspended using sonication, and the samples were stored at -20°C for up to 1 day prior to quantification. In order to quantify the total protein, samples were thawed, and thoroughly mixed. 2 µl of the sample were diluted in 500 µl DDW, to which 1 ml of Solution II was added (0.3 M Na Borate, 0.15% SDS, 5 mM CDTA [pH 9.2]). Following mixing, 1 ml of 0.06 M Fluorescamine ($C_{17}H_{10}O_4$) was added with vortexing, and the solutions were incubated for 3 minutes in the dark, at room temperature. Another 0.5 ml DDW was added, and the samples were incubated for 5 minutes (in the dark) at room temperature. Protein absorbencies of the samples and standards were measured by fluorescence spectrophotometry, at an excitatory wavelength of 390λ, and an emission wavelength of 475 λ using a LS-5 Fluorescence Spectrophotometer (Perkin Elmer, USA). Protein concentrations were determined via linear regression of the standard curves using GraphPad Prism version 3.02 for Windows (GraphPad Software, San Diego California USA, www.graphpad.com).

2.6 Cytotoxicity assay

The clonogenic procedure used was based on a methodology introduced by Dornish *et al.*, 1987. Briefly, cells were exposed to cisplatin (0.02, 0.04, 0.08, 1, 2, 3, 4, 5, 6, 7, 8, 10, 15, 20, 25, 30, 35, 40, 80 µg/ml) for 1 hour at 37°C. Cisplatin was supplied

as a 1 mg/ml clinical formulation, which consisted of 1 mg/ml sodium chloride and 9 mg/ml mannitol, and dilutions were prepared in sterile PBS. Following a one-hour drug exposure, the medium was removed, the cells were washed twice in PBS and were harvested by trypsinization. Between 300 and 30 000 cells (depending on the concentration of CP to which the cells had been exposed) from each flask were seeded into each of three cell culture dishes containing 5 ml of fresh medium. The dishes were then incubated until colonies of 60 cells were formed (approximately 11 days for the SBC-3 cells and 27 days for the Saos-2 cells). Following incubation, cells were stained with methyl blue to better visualize the colonies, and were counted. Cells that underwent the same treatment minus CP were plated and allowed to form colonies concurrently under the same conditions for use as negative controls.

In order to determine the effects of GCS inhibition on colony survival, SBC-3 cells were also exposed to 100 μM of BSO for 24 hours prior to the clonogenic assay. SBC-3/GCS cells were exposed to 10 μM or 100 μM of BSO for 24 hours prior to the clonogenic assay. In all cases, the cell culture medium was replaced with fresh medium (pre-warmed to 37°C) immediately prior to the addition of CP.

2.7 Data analysis of clonogenic survival data

Data were transformed, graphed, modelled and statistically analysed using GraphPad Prism version 3.02 for Windows (GraphPad Software, San Diego California USA, www.graphpad.com), and Microsoft Excel '97. In all cases, the data was normalized against a drug-free control value in each experiment, which is meant to

represent 100% survival. The data were then transformed to give a log effect (y-axis) vs. linear dose (x-axis), as is the convention for *in vitro* cancer survival curves. This transformation is also useful in examining the effects at high doses, which are of particular interest in studies of antineoplastic resistance. The data were modelled via non-linear regression, using a sigmoidal model based on the expression

$$Y = Bottom + \frac{(Top - Bottom)}{1 + e^{\left(\frac{LD50 - x}{Slope}\right)}}$$

Bottom = Lower asymptote of the Curve

Top = Upper Asymptote of the Curve

LD50 = Concentration of CDDP required to achieve 50% Clonogenic Survival

Slope = Slope during Logarithmic decrease in Clonogenic Survival

Parameters estimated by the curve fitting were obtained for each data set, and were compared between parent cells and their transfectants using an unpaired t-test ($p \leq 0.05$). In both cell lines, the fit converged for all data sets, where each replicate was considered individually, no weighting was used (minimize absolute distances squared), and convergence was reached when two consecutive iterations changed the sum-of-squares by less than 0.01%.

For the passive resistance model, the upper asymptote of the dose-response curve was fixed at 100% (log 2), as one would expect that at the lowest dose survival would approximate 100% and slight changes in survival at the lowest dose could be attributed to

experimental variance. An additional constraint was added for the active resistance model, where the lower asymptote was also fixed to a value approaching 0% survival.

For each clonogenic experiment, a dose-response curve was constructed, and the upper and lower asymptotes, as well as the LD50 and slope of the logarithmic cell-killing phase were recorded. The data collected for each experiment were used for statistical comparison. and were used to determine the mean values as well as the standard errors for each relevant parameter. The mean value for each point of the dose-response curve was used to construct the mean dose-response curve.

2.8 Solving dose-response curves for the points of inflection

Following the non-linear regression analysis of the clonogenic survival data, it was decided that solving the resultant curves for the inflection points would be helpful in a more accurate description of the data. The first and second derivative of the overall dose-response curve for each cell line/transfectant was determined, and the extrema (on the Y-axis) of the second derivative was determined. The second derivative was then solved at the extrema, to yield their co-ordinates on the x-axis. These co-ordinates corresponded to the x-axis values of the inflection points for the dose-response curve. A purely illustrative example is shown in Figure 4, where a sigmoid curve is plotted in red. Note that in this example, the Y axis is linear, while the X-axis is logarithmic. Consequently, the origin of the graph is centred on $X=Log_{10}(0)$, and the Y-intercept does not occur at 100% survival. Where the plot to be converted and graphed on a Log_{10} Y Linear X graph, the Y-intercept would occur where Y=100% survival, and the X-

intercept would occur at a drug concentration of 0 μg/ml. Although carried out manually at first, these calculations were subsequently performed using the Unix-based Maple V, release 5.1.

Figure 4: Determining inflection points. Following the estimation of the dose-response curve via non-linear regression, the second derivative is determined (purple line), and the extrema of that function are calculated (A) The second derivative of the function is then solved for x, where y = extrema. This provides the x-axis value (B) of the inflection point (C) of the corresponding dose-response curve (red). This figure is strictly for illustrative purposes, and does not approximate the derived dose-response curves.

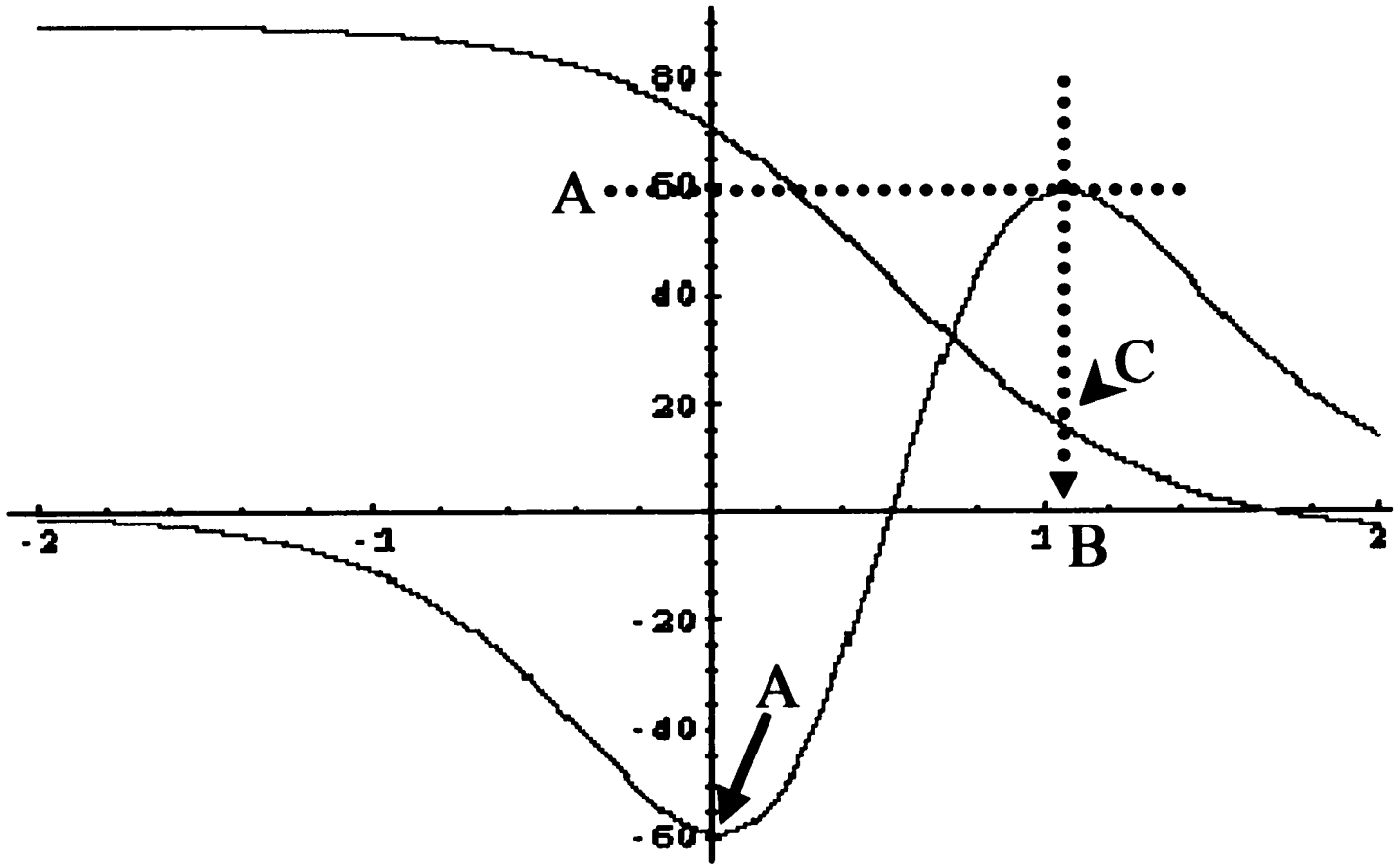
60
A
40
20
C
-2
-1
1
B
2
-20
A
-40
-60

3. RESULTS

3.1 Characterization of cell lines

3.11 Human osteosarcoma Saos-2, and its wild type p53 transfectant, Saos-2/p53

Two different cell lines were used in the analysis of our drug resistance hypothesis. One of these cell lines is Saos-2, a commercially available human osteosarcoma, whose characteristic of interest is the absence of endogenous p53. This cell line has a large, spread out morphology, and grows steadily to overconfluence. The doubling time of this cell line is approximately 41 hours during the logarithmic growth phase, and the cells are maintained in low-glucose Dulbecco's Minimum Essential Medium (Gibco Brl, USA), which is replaced every 2-3 days.

The wild-type p53 transfectant, Saos-2/p53, was obtained thanks to a generous donation by Dr. Kumio Okaichi (Atomic Bomb Disease Institute, Nagasaki, Japan). This transfectant was established via the transfection of a human wild-type p53 cDNA gene carried by a LacSwitch inducible mammalian expression system by Stratagene (La Jolla, CA., USA). The expression plasmid is pOP13(CAT), where the CAT gene was replaced by the p53 gene at the Not I sites. A plasmid of p3'SS which expressed the lac I gene encoding the lac repressor protein was used as the regulation plasmid. The expression of wild-type p53 was thus largely suppressed by the lac repressor. This repression can be removed by adding 5mM IPTG to the culture medium, which inhibits production of the lac repressor. The p53 transfected cell line (Saos-2/p53) was morphologically quite

similar to the parent cell line, although the doubling time of the cell line was somewhat slower (58 hours). This is believed to be due to the leaky nature of the double vector lacZ system used for the transfection, where a baseline level of wild-type p53 is produced (Okaichi *et al.*, 1998). Note that the term "leaky" refers to the low level of p53 product produced by this vector system, even when the promoter is repressed. Most interestingly, previous work with this cell line has shown that the "leaky" nature of this vector system is sufficient to induce cell cycle arrest and an apoptotic response to a toxic insult (Wang *et al.*, 1998). When p53 production is fully induced by IPTG, the doubling time of Saos-2/p53 increases to almost 106 hours. For the purposes of our work, it was helpful to select for non-transfected Saos-2 cells from the Saos-2/p53 population. We were able to obtain these cells via long term exposure of the Saos-2/p53 population to 5 mM IPTG. We have named these cells Saos-2/p53-, to signify that they originate from the Saos-2/p53 population, but do not contain any detectable p53 gene product.

Figure 5: Western Blotting of Saos-2 (A) and SBC-3 (B) cell lines, and their transfected variants. A)Saos-2/p53 cells were exposed to 5mM IPTG for 24 hours prior to p53 detection in order to induce high level expression, by way of a lacSwitch recombinant double vector system. The cells were lysed, and proteins were extracted as described. The proteins of interest were selected via immunolabelling with specific antibodies, and were subsequently detected via exposure to secondary antibodies conjugated to horseradish peroxidase. B) SBC-3 cells were lysed, and proteins were extracted as described. The proteins of interest were selected via immunolabelling with specific antibodies, and were subsequently detected via exposure to secondary antibodies conjugated to horseradish peroxidase.

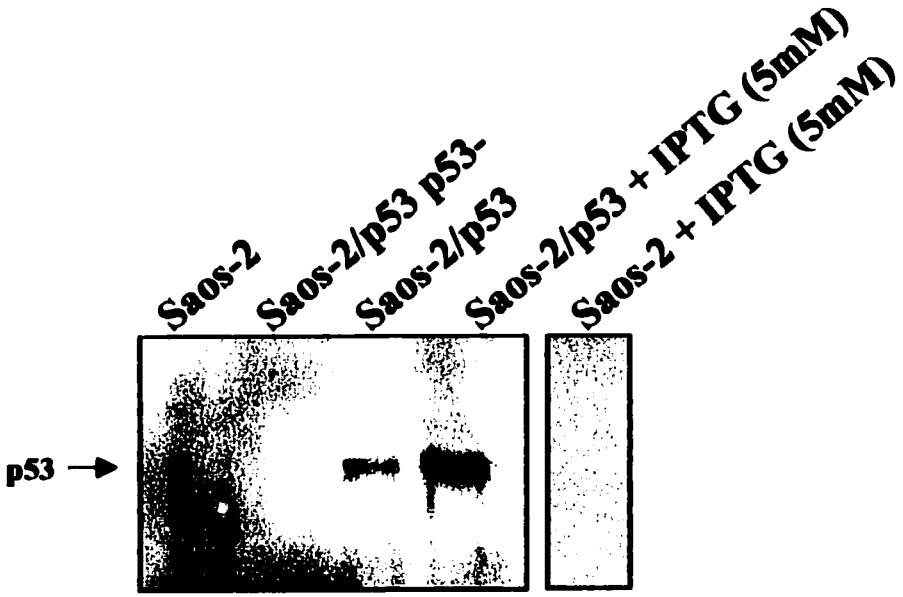
Saos-2
Saos-2/p53 p53-
Saos-2/p53
Saos-2/p53 + IPTG (5mM)
Saos-2 + IPTG (5mM)
p53

A

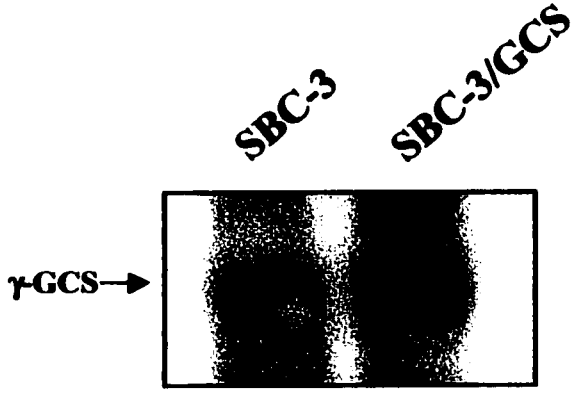
SBC-3
SBC-3/GCS
γ-GCS

B

Figure 6: Relative differences in protein quantity in transfected cell lines compared to the parent in A) Saos-2 cells, and the B) SBC-3 cell line, determined from western blotting image analysis. The x-ray films were scanned and quantified using the ImageQuant software (v. 4.2a Build 13).

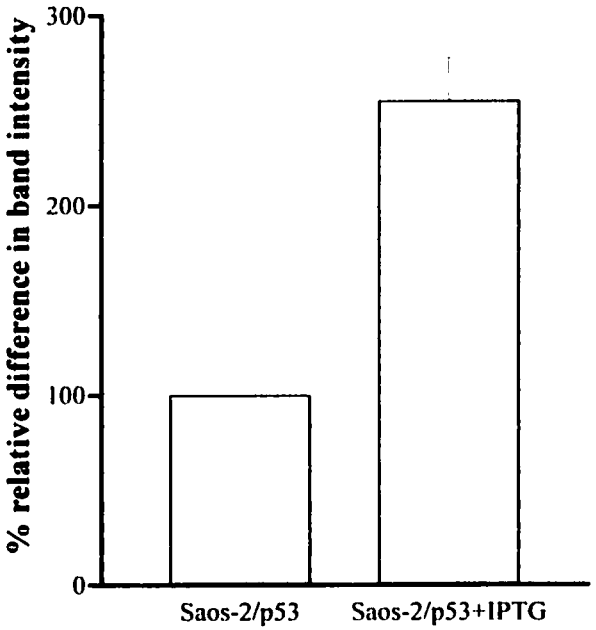
% relative difference in band intensity
300
200
100
0
Saos-2/p53
Saos-2/p53+IPTG

A

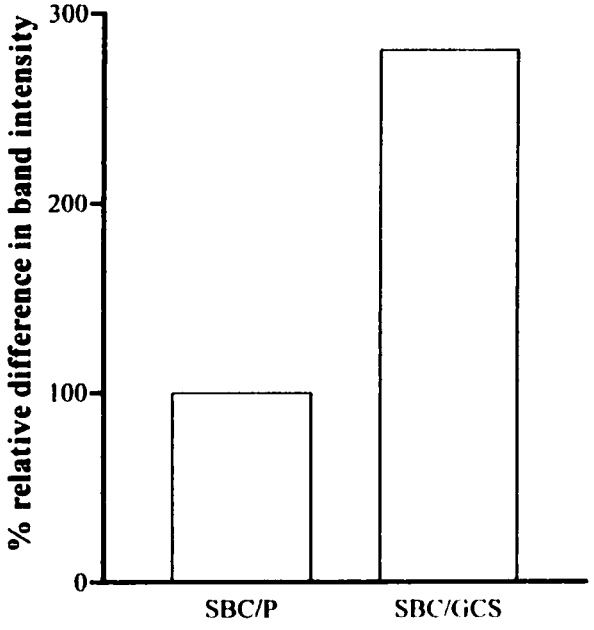
% relative difference in band intensity
300
200
100
0
SBC/P
SBC/GCS

B

3.12 Human small-cell lung cancer SBC-3 and its γ-GCS transfectant, SBC-3/GCS

The SBC-3 cell line, the second cell line used in our investigation, is a human small-cell lung cancer. Its transfectant, SBC-3/GCS, contains the full length coding region of the γ-GCS, which has been sub-cloned into the TA cloning site of the eukaryotic expression vector pCR3. Both cells are considerably smaller than the Saos-2 line, and have a rounder morphology. The doubling time of these cells are virtually identical (20 hours for SBC-3, 25 hours for SBC-3/GCS). Both SBC-3 and SBC-3/GCS were generously provided by Dr. Kazuto Nishio (National Cancer Research Institute, Tokyo, Japan).

3.2 Presence of p53 in Saos-2/p53 cells, and γ-GCS in SBC-3/GCS cells

i) Saos-2/p53 cells

Western blotting of Saos-2 cells revealed the presence of wild-type p53 in high abundance in the Saos-2/p53 cells following 24 hour exposure to 5mM IPTG. Exposure of the parent Saos-2 cell line to 5 mM of IPTG did not result in any visualization of a signal (Figure 5). Image analysis of the resultant blots revealed significant differences in signal intensity, where a 212±23.1% increase in p53 was observed in transfected cell that were induced with IPTG, when compared to Saos-2/p53 cells that were not induced (Figure 6 A; p=0.0214).

ii) SBC-3/GCS cells

Western blotting of SBC-3 and SBC-3/GCS cells stained for γ-GCS revealed a higher abundance of the enzyme in the transfectant. Significant differences were also observed in the SBC-3 cell line, with a 272.3±14.9% increase in γ-GCS detected in SBC-3/GCS cells, when compared to the SBC-3 parent cell line (Figure 6 B; p=0.0067).

3.3 Flow Cytometric analysis

Following the western blotting assay, we wished to determine the effects of wild-type p53 expression in Saos-2/p53 cells on the distribution of the cell population in the cell cycle. We also wanted to determine and any effects that GCS transfection might have on the cell cycle distribution of SBC-3 cells.

i) Saos-2, Saos-2/p53 and Saos-2/p53- cells

Saos-2, Saos-2/p53- cells and their Saos-2/p53 transfectants were exposed to cisplatin (4μg/ml) for one hour, incubated to allow recovery for 24 hours, and then analysed via flow cytometry (Figure 7, Table 1). Saos-2 control cells and Saos-2/p53- cells were found to have a similar proportion of cells in $G1/G_0$, and these values did not deviate from each other significantly. When exposed to cisplatin, the proportion of cells in $G1/G_0$ dramatically decreased in both the Saos-2 and the Saos-2/p53- cell line, with approximately 60% of the population found to be in the S phase (Table 1, Figure 7 B & F). Conversely, Saos-2/p53 had a much higher proportion of cells in the $G1/G_0$ phase

than either Saos-2 or Saos-2/p53- (Table 1, Figure 7 A, p=0.0534, p=0.0011, respectively), and this was found to decrease much less drastically when these cells were exposed to cisplatin (p=0.0172, p=0.0231, respectively). The number of Saos-2/p53 cells in the S phase was found to be significantly less than either the Saos-2 or the Saos-2/p53- population, following exposure to cisplatin (p=0.0358, p=0.0328, respectively). In all cases, the percentage of the population of cells in G2/M was not found to differ significantly.

A comparison of Saos-2/p53- cells to the parent cell line revealed a similar profile to the Saos-2 population in terms of cell cycle distribution (Table 1, Figure 7 A-D). Although there were minor variations in the cell cycle profiles of Saos-2 cells and Saos-2/p53- cells (i.e. the proportion of cells in G_1/G_0), there fluctuations were not statistically significant.no significant differences observed in $G1/G_0$ following exposure to cisplatin. The dramatic increase noted in the number of Saos-2 cells found in S phase following cisplatin treatment was paralleled in Saos-2/p53- cells, and any minor variances were not found to be statistically significant. As before, the G2/M phase remained relatively unchanged following cisplatin treatment, with no statistically significant changes detected.

Table 1: Distribution (%) of Saos-2, Saos-2/p53- and Saos-2/p53 cells in phases of the cell cycle ±1 hour exposure to cisplatin (±SE)

	Saos-2	Saos-2 + CP	Saos-2/p53-	Saos-2/p53- + CP	Saos-2/p53	Saos-2/p53 + CP
$G1/G_0$ (%)	55.8 ± 3.2	32.24 ± 3.26	48.8 ± 0.1	25.3 ± 1.1	64.93 ± 2.08	48.03 ± 4.74
S (%)	30.0 ± 1.72	57.54 ± 3.28	37.7 ± 0.4	64.1 ± 0.51	25.75 ± 0.85	44.62 ± 4.4
G2/M (%)	14.2 ± 1.62	10.23 ± 1.51	14.1 ± 0.25	10.67 ± 0.8	9.33 ± 1.44	7.36 ± 1.39

n=10

Figure 7: Flow cytometry histograms of Saos-2 cells and their p53 transfectants (Saos-2/p53), indicating changes in the distribution of cells in the cell cycle ± cisplatin (4.0 μg/ml for 1 hour), based on propidium staining of DNA. Saos-2 cells and their transfectants were collected in the log growth phase either as drug-free controls (A, C, E), or following 24 hour exposure to 4μg/ml cisplatin (B, D, F). The cells were fixed in cold ethanol, and stored at -20°C. Prior to flow cytometric analysis, the cells were collected, rinsed in saline solution (PBS), exposed to RNAase, and stained with a 25 μg/ml of propidium iodide. Flow cytometry was conducted at a low flow rate until 50 000 events were registered, and the resultant data file was analysed using MulticycleAV (v. 3.11).

Please note that the flow cytometry assays for the Saos-2/p53- cell line was conducted at a later time than the Saos-2 and the Saos-2/p53 cells. Between the time that the Saos-2 cells and the Saos-2/p53 cells were assayed, and the Saos-2/p53- cells were assayed, significant repairs were made to the flow cytometer. These repairs had an overall effect of compacting the cell cycle profile, but proportionally these results were nonetheless comparable to the data obtained for the parent and the transfectant cells.

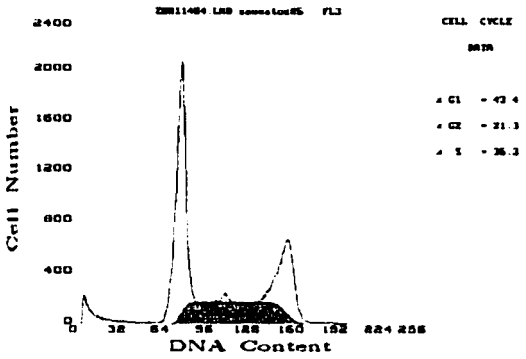

A) Saos-2

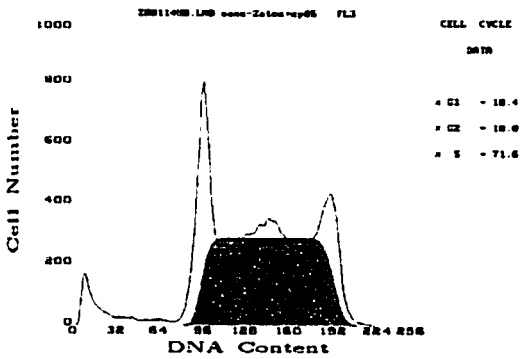

B) Saos-2 + CP

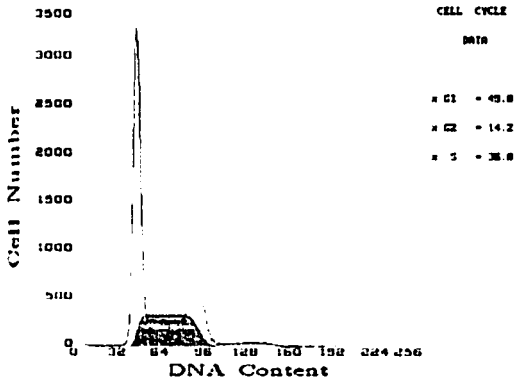

C) Saos-2/p53^{-}

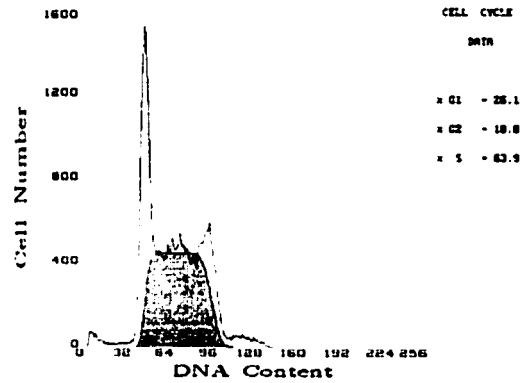

D) Saos-2/p53^{-} + CP

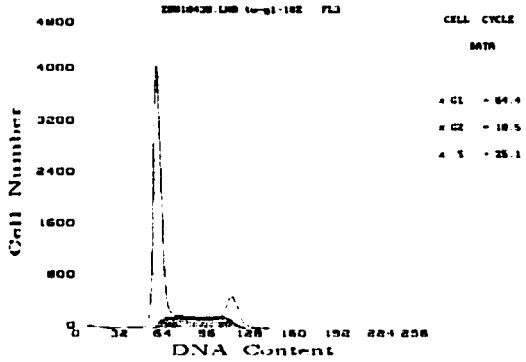

E) Saos-2/p53

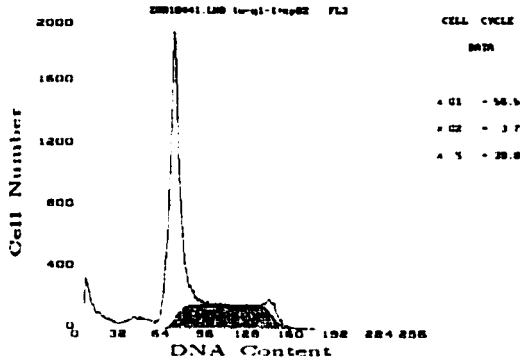

F) Saos-2/p53 + CP

ii) SBC-3 and SBC-3/GCS

Flow cytometric analysis of the SBC-3 cell line revealed less dramatic differences in cell cycle distribution. SBC-3 and SBC-3/GCS cells that were not exposed to cisplatin appeared to be quite similar in their cell cycle distribution profiles, with no significant differences detected in any phases of the cell cycle (Table 2, Figure 8 A-D). No significant differences were detected between the parent and transfected cell lines after exposure to cisplatin, however, differences in cell cycle distribution were detected in regards to each cell line relative to the drug-free control (Table 2, Figure 8 A vs. B, and C vs. D). Following 1 hour exposure to cisplatin, a significant difference in the G1 phase of SBC-3 when compared to the drug free control ($p=0.0206$) was detected. No significant difference was detected, however, in the G1 phase of SBC-3/GCS cells exposed to cisplatin, when compared to the drug free control.

Table 2: Distribution (%) of SBC-3 and SBC-3/GCS cells in phases of the cell cycle ±1 hour exposure to cisplatin (±SE)

	SBC-3	SBC-3 + CP	SBC-3/GCS	SBC-3/GCS + CP
$G1/G_0$ (%)	50.06 ± 2.22	46.26 ± 2.31	47.56 ± 1.80	44.38 ± 0.58
S (%)	36 ± 1.57	33.40 ± 0.93	35.99 ± 1.21	34.17 ± 1.0
G2/M (%)	13.95 ± 1.56	20.34 ± 2	18.04 ± 2.04	21.43 ± 1.11

n=6

3.4 Measurement of reduced glutathione in SBC-3 and SBC-3/GCS cells

Measurement of intracellular reduced glutathione in SBC-3 cells and their γ-GCS transfectants also revealed significant differences, where reduced GSH levels were found

to be elevated almost two-fold in the transfectants (Table 3, Figure 9; p=0.0036). Depletion of intracellular GSH levels occurred after 1 hour exposure to cisplatin in both SBC-3 and SBC-3/GCS cells; however, the overall levels of GSH were still found to be higher in the transfected cell line (Table 3, Figure 9).

Figure 8: Flow cytometry histograms of SBC-3 cells and their γ-GCS transfectants, indicating changes in the distribution of cells in the cell cycle ± cisplatin (0.8 μg/ml for 1 hour), based on propidium iodide staining of DNA. SBC-3 cells and their transfectants were collected in the log growth phase either as drug-free controls (A, C), or following 24 hour exposure to 0.8 μg/ml cisplatin (B, D). The cells were fixed in cold ethanol, and stored at -20°C. Prior to flow cytometric analysis, the cells were collected, rinsed in saline solutions (PBS), exposed to RNAase, and stained with a 25 μg/ml of propidium iodide. Flow cytometry was conducted at a low flow rate until 50 000 events were registered, and the resultant data file was analysed using MulticycleAV (v. 3.11).

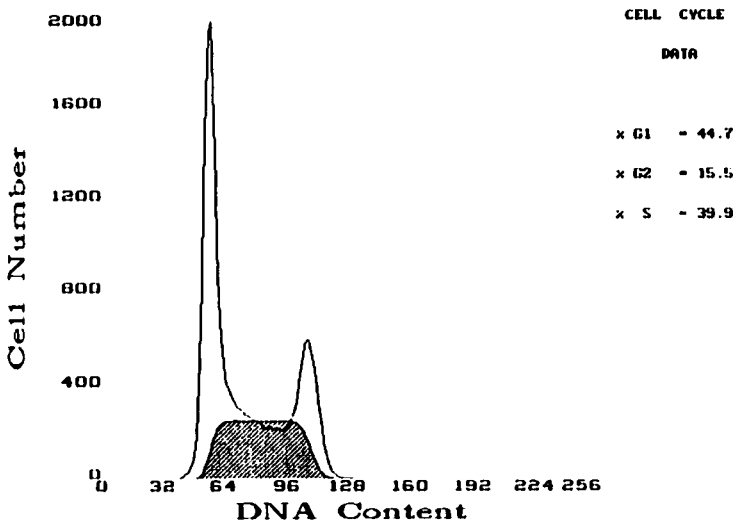

A) SBC-3

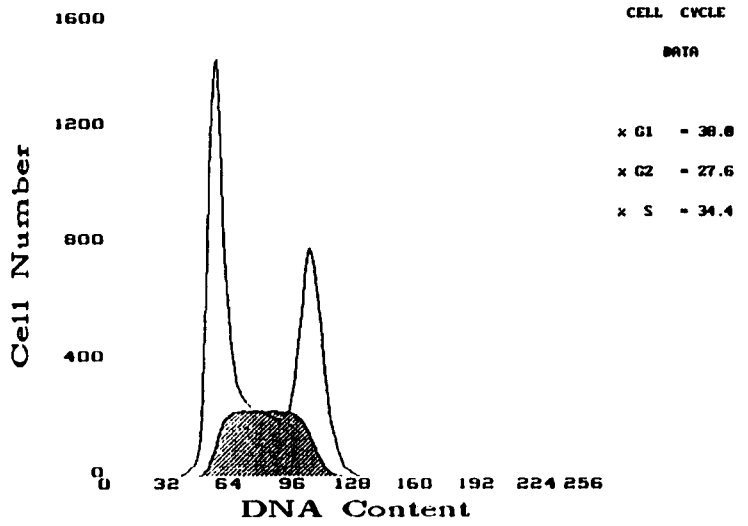

B) SBC-3 + Cisplatin

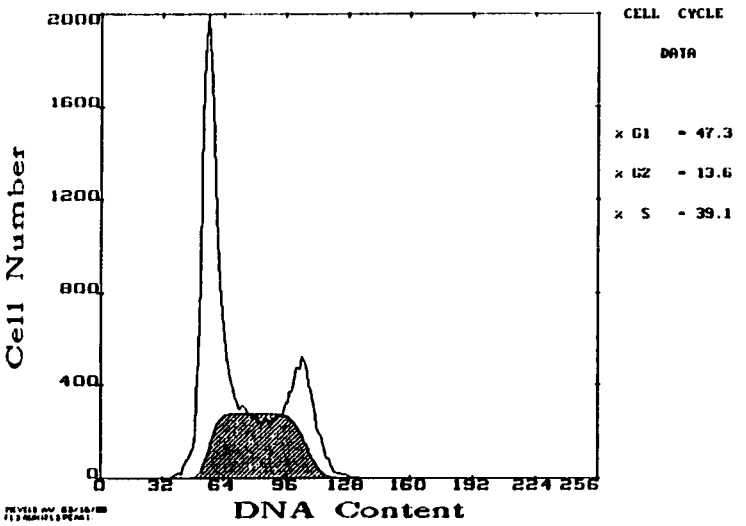

C) SBC-3/GCS

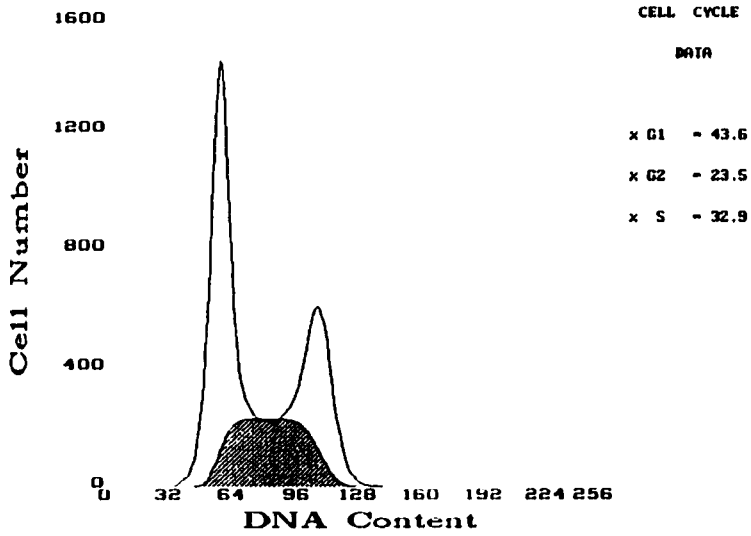

D) SBC-3/GCS + Cisplatin

Figure 9: Intracellular GSH concentrations in SBC-3 cells, and their transfectants. A) Intracellular reduced glutathione concentrations (GSH) in SBC-3 and SBC-3/GCS cells ± 0.8μg/ml cisplatin. B) Intracellular reduced glutathione concentrations (GSH) in SBC-3 and SBC-3/GCS cells ± BSO. Following treatment with cisplatin or BSO, cells were collected and lysed in 2N perchloric acid. The supernatant was removed, and neutralized in 2N KOH. The supernatant was then stained with 1mg/ml o-Phthaldehyde, and the resultant fluorescence was quantified via fluorescent spectroscopy. These values were normalized to total protein quantification of each sample. Regression analyses were carried out using GraphPad Prism (v. 3.02). Note that the error bars indicate standard errors (n = 4).

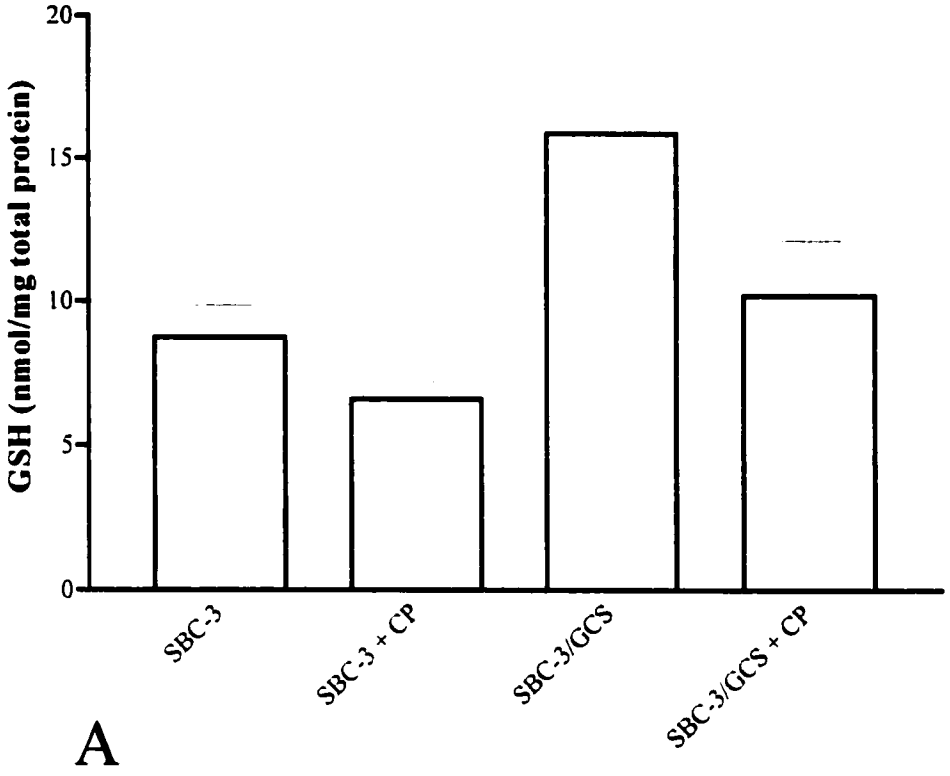
GSH (nmol/mg total protein)
20
15
10
5
0
SBC-3
SBC-3 + CP
SBC-3/GCS
SBC-3/GCS + CP

A

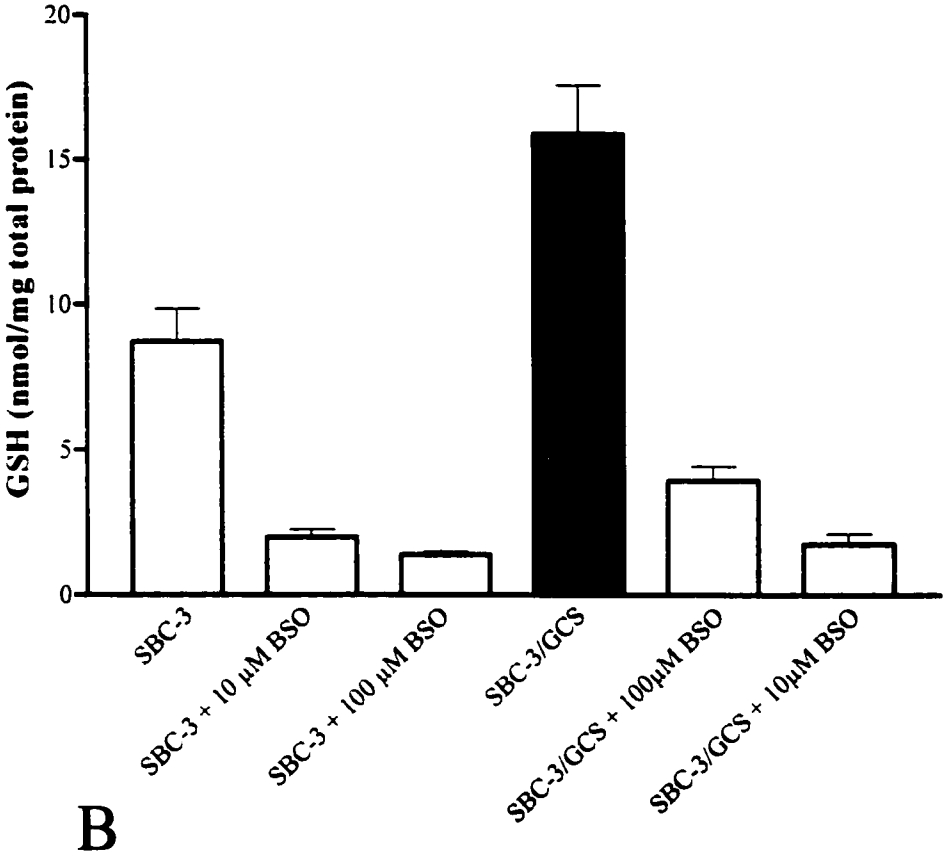
GSH (nmol/mg total protein)
20
15
10
5
0
SBC-3
SBC-3 + 10 μM BSO
SBC-3 + 100 μM BSO
SBC-3/GCS
SBC-3/GCS + 100μM BSO
SBC-3/GCS + 10μM BSO

B

Table 3: Comparison of intracellular reduced glutathione in SBC-3 & SBC-3/GCS cells ± Cisplatin (SE) for 1 hour @ 0.08 µg/ml

	SBC-3	SBC-3 + CP	SBC-3/GCS	SBC-3/GCS + CP
GSH (nmol/mg)	8.74 ± 1.14	6.60 ± 0.60	15.9 ± 1.70	10.23 ± 1.93

n = 4

Following exposure to buthionine sulfoximine (BSO), which functions as a specific and otherwise non-toxic inhibitor of γ-GCS, GSH levels were found to drop in both the parent and transfected cell lines. Following a 24 hour exposure to 10 µM BSO, GSH levels dropped in both SBC-3 and GCS cells, however, levels of GSH were still more than two-fold higher in GCS cells than in the parent cell line (Table 4, Figure 9b; p=0.0298). GSH levels were found to be similar in SBC-3 and GCS cells following 24 hour exposure to 100 µM BSO, with no statistically significant differences (Table 4; Figure 9b).

Table 4: Comparison of intracellular reduced glutathione in SBC-3 & SBC-3/GCS cells ± BSO (SE) for 24 hours @ 10, or 100 µM

	SBC + 10µM	SBC-3 + 100 µM	GCS + 10 µM	GCS + 100 µM
GSH (nmol/mg)	1.9±.28	1.39±0.098	3.95±0.52	1.75±0.37

n = 4

3.5 Clonogenic dose-response curves

3.51 The effects of cisplatin on colony survival of Saos-2, Saos-2/p53- and Saos-2/p53 cells

Saos-2 cells were found to respond to cisplatin treatment, and displayed a sigmoid dose-response relationship with escalating concentrations of the drug (Figure 10 curve A). Although able to maintain a near-100% survival at low doses of cisplatin up to approximately 1 μg/ml, subsequently there was a rapid, logarithmic decline in the surviving population up to approximately 15 μg/ml. The terminal plateau of the dose-response curve that appeared at 15 μg/ml persisted at high doses up to 40 μg/ml (Table 5), and there was very little decrease in the number of cells that were able to survive cisplatin concentrations within this range (Figure 10 curve A).

Saos-2/p53- cells that were exposed to the same conditions were found to share a somewhat similar profile to that of the Saos-2 cell line. Near-maximal levels of survival were maintained up to 1 μg/ml, followed by a rapid and logarithmic decline up to 15 μg/ml (Figure 10 curve B). There was a resistant terminal plateau, which persisted up to 40 μg/ml (Figure 10 curve B). Although a slight difference was observed between the terminal plateau of Saos-2/p53- and the parent Saos-2 cell line, this difference was not statistically significant. The slope of the dose-response curve did not change appreciably relative to the parent cell line, and the variance was not significant (Table 5). Furthermore, the LD_{50}, although somewhat lower than the Saos-2 cell line, did not differ significantly when compared to the parent (Table 5).

Saos-2/p53 cells exposed to low doses of cisplatin followed a similar trend to the Saos-2 and Saos-2/p53- cell line, where colony survival approached 100% up to 1 μg/ml. The LD_{50} and slope did not vary significantly from either the parent or the Saos-2/p53- cell line (Table 5). As noted in the parent and Saos-2/p53- cell lines, a logarithmic decrease in colony survival was observed between 1 and 15 μg/ml (Figure 10 curve C). This trend continued in the Saos-2/p53 cells, however, up to approximately 25 μg/ml after which a terminal plateau containing the most resistant cells was found (Figure 10 curve C). The terminal plateau differed significantly from the parent cell line, as well as from Saos-2/p53- cells ($p=0.001$ and $p=0.007$, respectively).

Figure 10: Clonogenic dose-response curves of Saos-2 (black line), Saos-2/p53- (dashed line) and Saos-2/p53 (red line) cells following 1 hour exposure to cisplatin. The insert displays the dose-response curve with the x-axis converted to log values, to more easily discriminate the shape of the curve at low concentrations of cisplatin, and is for illustrative purposes only. Briefly, cells in the log phase of growth were exposed to cisplatin for 1 hour (0.02-40 μg/ml). The drug-containing media was aspirated, and the cells were washed with saline solution (PBS). Following trypsinization, the concentration of cells were determined for each sample, and an appropriate number were plated into clonogenic plates (300-30 000, depending on the concentration of cisplatin to which the cells were exposed). Colonies of 60 cells were allowed to form, after which the clonogenic plates were stained with methyl blue. Colonies were then counted, and colony survival was normalized against a drug-free control. Subsequent analysis of the dose-response profile using non-linear regression resulted in an estimation of the dose response curve.

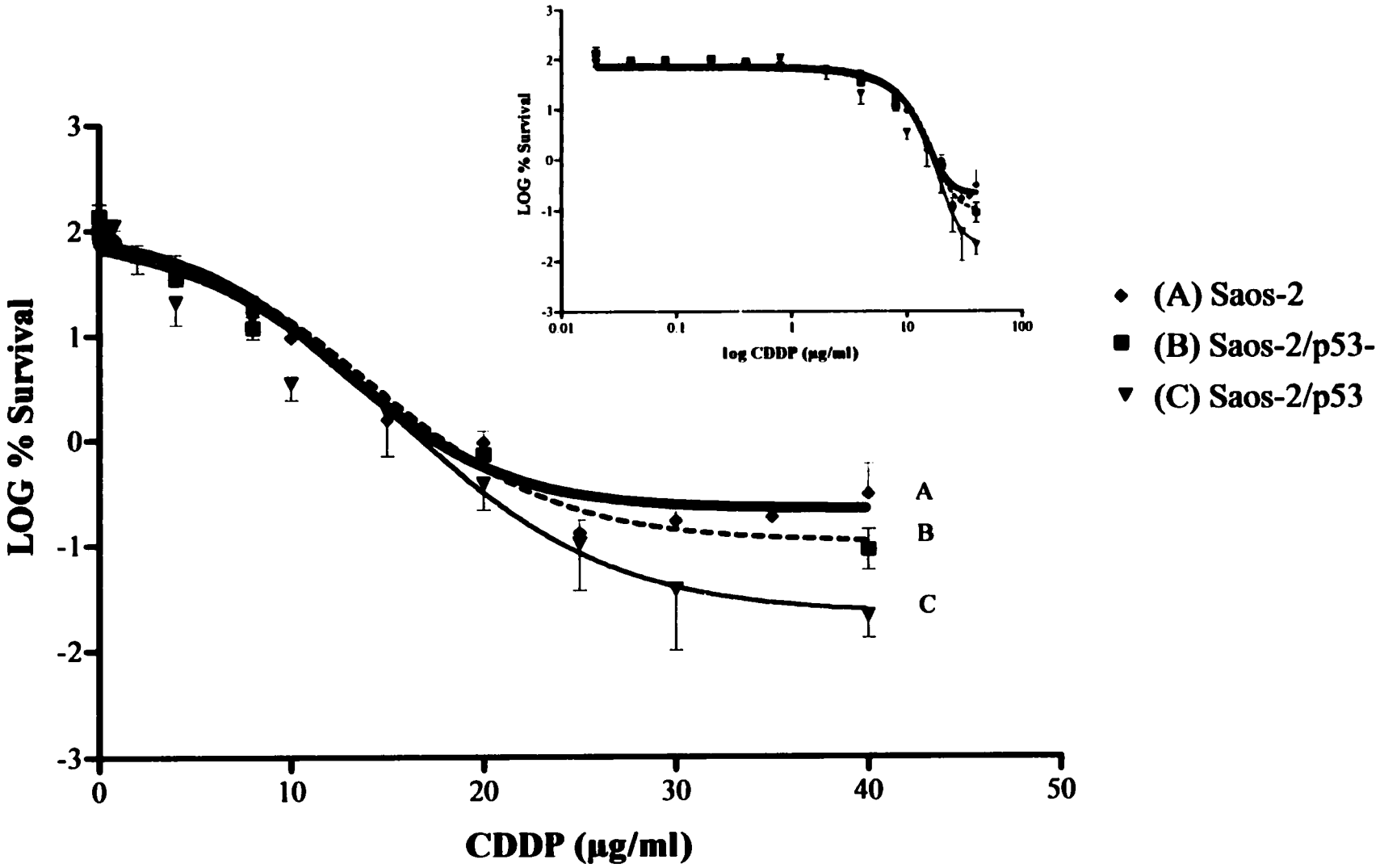
LOG % Survival
3
2
1
0
-1
-2
-3
0
10
20
30
40
50
CDDP (µg/ml)
A
B
C
LOG % Survival
log CDDP (µg/ml)
0.01
0.1
1
10
100
(A) Saos-2
(B) Saos-2/p53-
(C) Saos-2/p53

Table 5: Comparison of Saos-2, Saos-2/p53- and Saos-2/p53 dose-response curve parameters as estimated via non-linear regression (±SE)

	Saos-2	Saos-2/p53-	Saos-2/p53
LD_{50} (µg/ml)	15.78 ± 1.18	14.37 ± 1.137	15.78 ± 1.177
Slope	-4.3 ± 0.44	-4.91 ± 0.75	-5.52 ± 0.47
Terminal Plateau (%)	0.17 ± 0.021	0.11 ± 0.017	0.089 ± 0.011

n=6

3.52 The effects of cisplatin on the colony survival of SBC-3 and SBC-3/GCS cells ± BSO

SBC-3 cells responded to cisplatin treatment in a sigmoid fashion, where colony survival approaching 100% was observed up to approximately 1 µg/ml, followed by a steep and logarithmic decline in surviving cells, ending with a terminal plateau at 10 µg/ml (Figure 11; solid line). In the case of SBC-3/GCS cells, colony survival approached 100% for the entire low-dose plateau observed for the SBC-3 cells, and extended further up to approximately 2 µg/ml (Figure 11, red). A logarithmic decline in colony survival was observed in the SBC-3/GCS cells up to approximately 15 µg/ml, followed by a terminal plateau (Figure 11). Correspondingly, significant differences were observed between the LD50 values of SBC-3 and SBC-3/GCS cells (Table 6; p= 0.0001). The steepness of the slope was also found to differ significantly between SBC-3 and SBC-3/GCS cells (Table 6; p=0.0001).

Figure 11: Dose-response curves of SBC-3 (black line) and SBC-3/GCS (red line) cells following 1 hour exposure to cisplatin. The insert displays the dose-response curve with the x-axis converted to log values, to more easily discriminate the shape of the curve at low concentrations of cisplatin, and is for illustrative purposes only. Briefly, cells in the log phase of growth were exposed to cisplatin for 1 hour (0.02-40 μg/ml). The drug-containing media was aspirated, and the cells were washed with saline solution (PBS). Following trypsinization, the concentration of cells was determined for each sample, and an appropriate number were plated into clonogenic plates (300 - 30 000, depending on the concentration of cisplatin to which the cells were exposed). Colonies of 60 cells were allowed to form, after which the clonogenic plates were stained with methyl blue. Colonies were then counted, and colony survival was normalized against a drug-free control. Subsequent analysis of the dose-response profile using non-linear regression resulted in an estimation of the dose response curve.

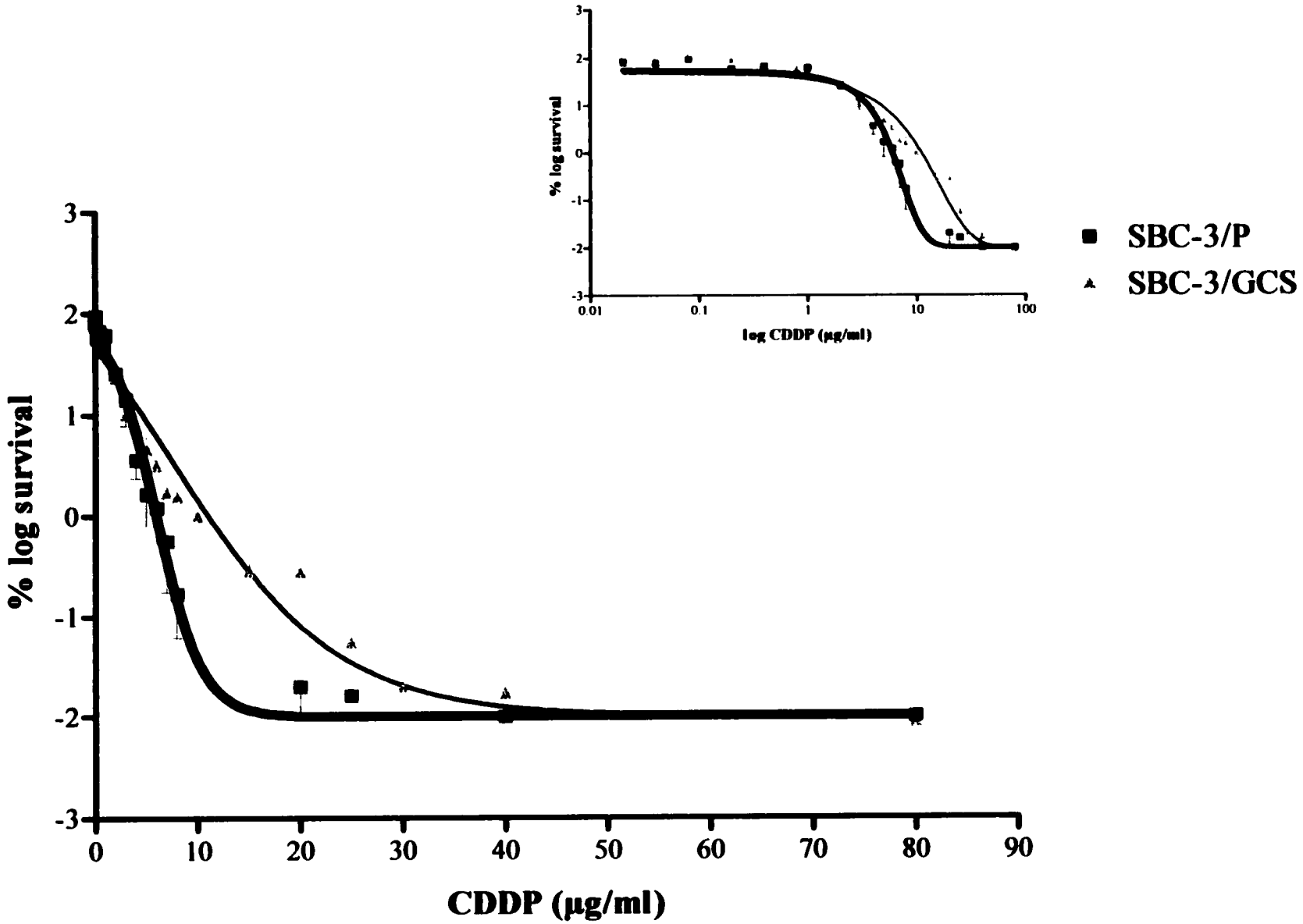
% log survival
CDDP (μg/ml)
SBC-3/P
SBC-3/GCS
log CDDP (μg/ml)

3.53 The response of SBC-3/GCS cells to cisplatin following the inhibition of glutathione synthesis using BSO

Following a 24 hour exposure to BSO, SBC-3/GCS cells were analysed for their response to cisplatin treatment via a clonogenic assay (Figure 12, Table 6). In all cases, colony survival approached 100% at low doses. Differences were observed, however, in terms of the estimated LD_{50} and slope of the dose-response curve. SBC-3/GCS and SBC-3 cells exposed to 100 μM of BSO demonstrated the highest sensitivity to escalating concentrations of cisplatin, with a correspondingly low LD_{50} (Table 6, Figure 13 [B, C, D; yellow and blue lines, respectively]). These LD_{50}s were lower than the LD_{50} of SBC-3/GCS cells exposed to 10 μM of BSO (Figure 13 [A, D; orange line]). The dose-response curve of SBC-3/GCS (without BSO) cells had a much higher LD_{50} than all other clonogenic dose-response curves obtained for the SBC-3 cell line (Figure 13 [D; red line]), and it differed significantly from clonogenic assays carried out on SBC-3/GCS cells exposed to either 10 μM and the 100 μM BSO inhibition assays ($p<0.0001$ in all cases). The LD_{50} of SBC-3/GCS cells exposed to 100 μM of BSO was found to be considerably lower than the LD_{50} of SBC-3 cells ($p=0.0018$), but SBC-3/GCS cells exposed to 10 μM BSO were not found to differ significantly from SBC-3 cells.

Figure 12: Dose-response curves for SBC-3/GCS cells with and without BSO, following 1 hour exposure to cisplatin. The dose-response curve of SBC-3/GCS is represented by a red line. SBC-3/GCS cells exposed to 10 μM BSO are represented by an orange line, and SBC-3/GCS cells exposed to 100 μM BSO are represented by a yellow line. The clonogenic assay was carried out as previously described, with the addition of buthionine sulfoximine for 24 hours prior to drug treatment. The insert displays the dose-response curve with the x-axis converted to log values, to more easily discriminate the shape of the curve at low concentrations of cisplatin, and is for illustrative purposes only.

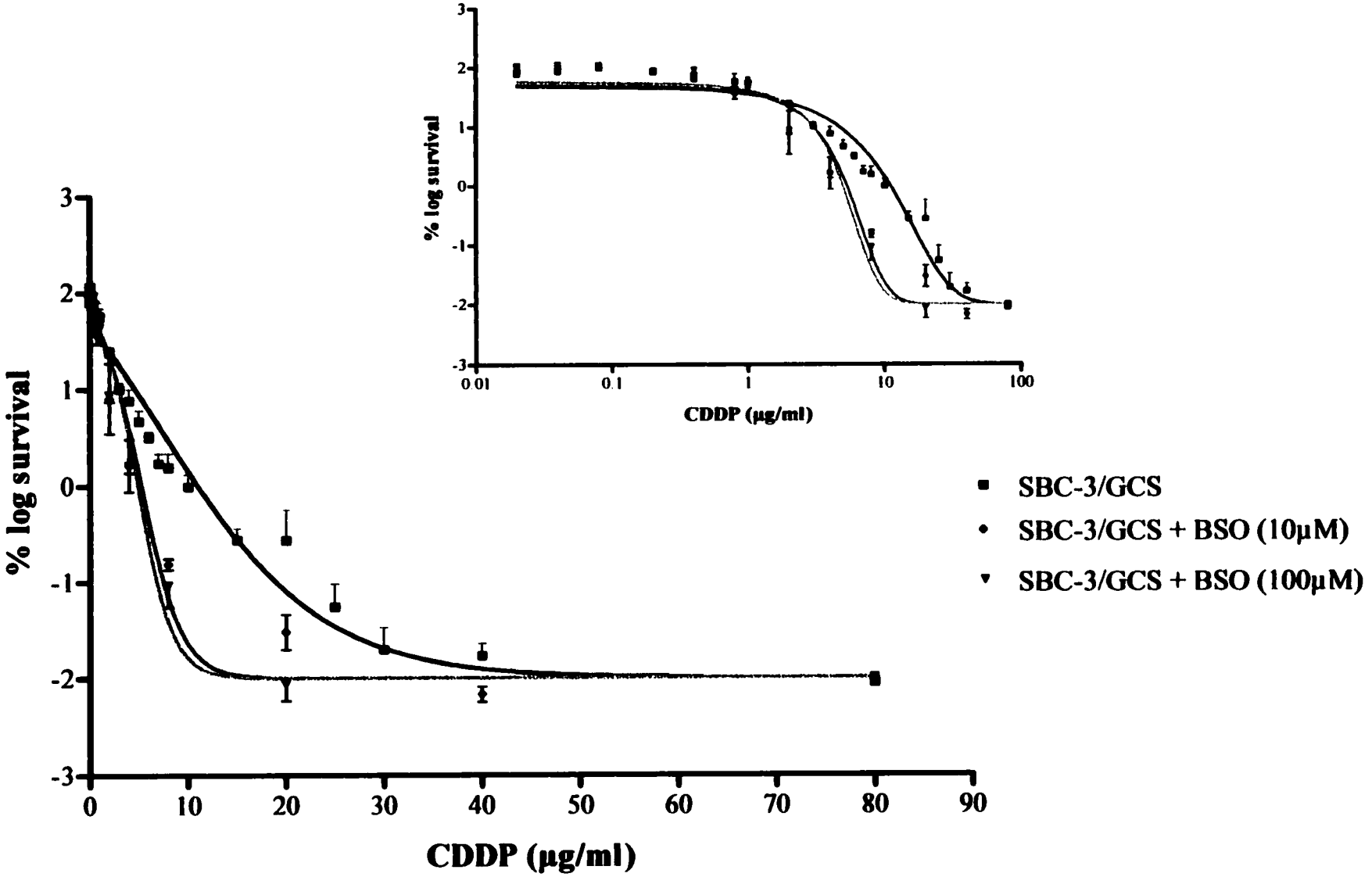
% log survival
CDDP (μg/ml)
SBC-3/GCS
SBC-3/GCS + BSO (10μM)
SBC-3/GCS + BSO (100μM)

The slope of the dose-response curve in the BSO inhibition assays was found to decrease significantly in relation to the BSO-free experiments ($p<0.0001$ in all cases). The slope of the dose-response curve obtained for SBC-3/GCS cells exposed to 100 μM of BSO was also significantly more steep than the slope obtained for SBC-3 cells ($p=0.0239$). The slope of SBC-3/GCS cells exposed to 10 μM of BSO did not, however, differ significantly from the slope obtained for SBC-3 cells (Table 6, Figure 13). The LD_{50} of SBC-3 cells exposed to 100 μM BSO also differed significantly from SBC-3 cells not exposed to BSO ($p=0.004$).

Table 6: Comparison of SBC-3 & SBC-3/GCS dose-response curve parameters, and of SBC-3 & SBC-3/GCS dose-response curve parameters following 24 hour exposure to BSO (±SE), as estimated via non-linear regression

	Clonogenic Assays (without BSO)		Clonogenic Assays with 10 or 100 100 μM BSO		
	SBC-3	SBC-3/GCS	SBC-3 + 100 μM	SBC-3/GCS + 10 μM	SBC-3/GCS + 100 μM
LD_{50} (μg/ml)	6.27 ± 29.0	8.12 ± 13.0	4.4 ± 0.37	5.3 ± 0.4	4.95 ± 0.27
Slope	-3.23 ± 83.0	-2.16 ± 81.0	-1.76 ± 0.25	-2.06 ± 0.26	-1.76 ± 0.17

n=8

Figure 13: Dose-response curves for SBC-3 cells (black, blue lines) and SBC-3/GCS cells (red, orange, yellow lines). A) SBC-3/GCS cells exposed to 10 μM BSO. B) SBC-3/GCS cells exposed to 100 μM BSO. C) SBC-3 cells exposed to 100 μM BSO. D) A comparison of all dose response curves. The clonogenic assay was carried out as previously described, with the addition of buthionine sulfoximine for 24 hours prior to drug treatment. The insert displays the dose-response curve with the x-axis converted to log values, to more easily discriminate the shape of the curve at low concentrations of cisplatin, and is for illustrative purposes only.

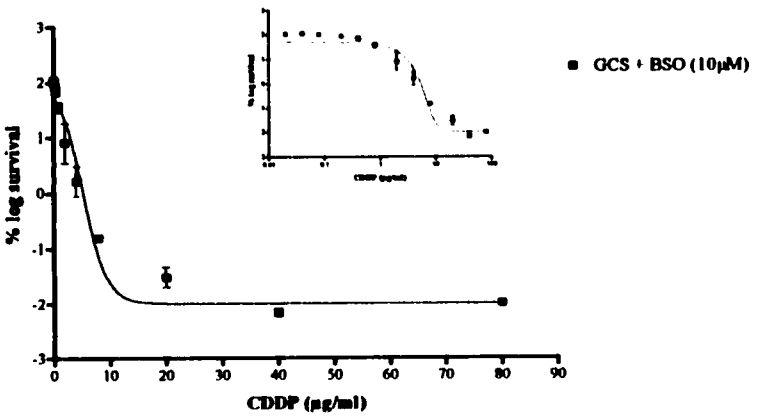

A) SBC-3/GCS + 10 μM BSO

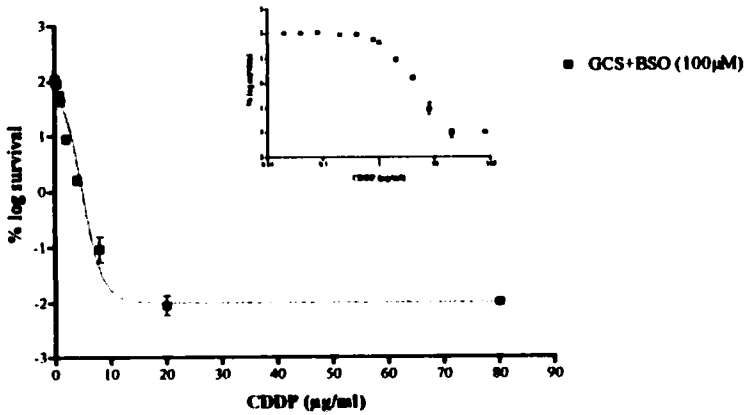

B) SBC-3/GCS + 100 μM BSO

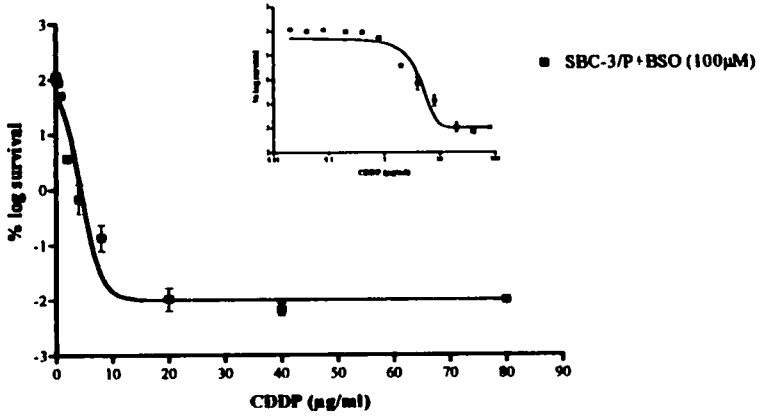

C) SBC-3 + 100 μM BSO

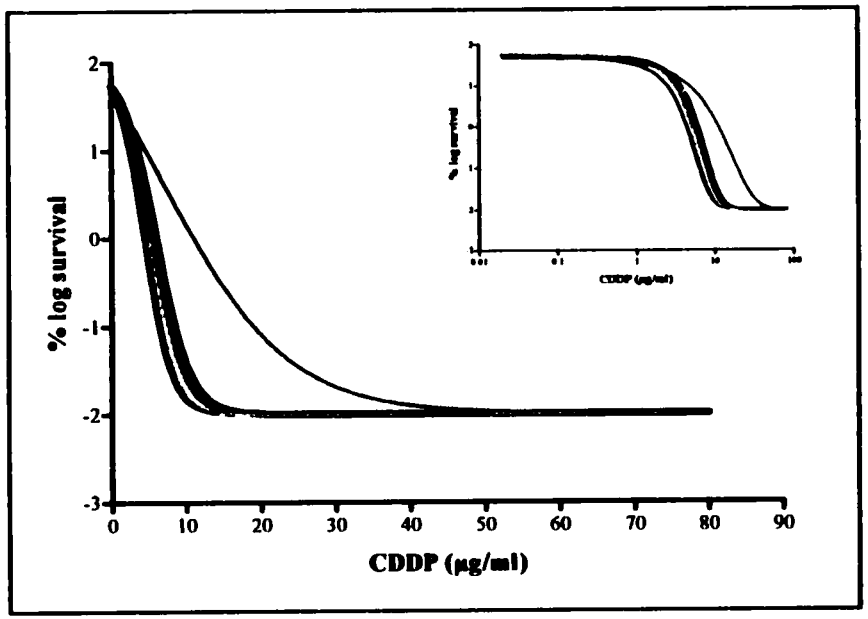

D) SBC-3 & SBC-3/GCS ± BSO

3.54 The derivatization of the inflection points, and determination of their values

i) SBC-3 and SBC-3/GCS cells

Characterization of the dose-response curves indicated trends that were consistent with changes in the LD_{50} and slope. SBC-3 cells had a shoulder on the curve, with an inflection point at 3.1 μg/ml, followed by another inflection point at 8.9 μg/ml (Table 7). SBC-3/GCS cells were found to have the first inflection point at a higher dose of cisplatin, and the second inflection point was found to occur at a much higher dose than that for SBC-3 (Table 7). Inhibition of GSH synthesis with BSO had the opposite effect, where inflection points at low doses were found to occur at lower concentrations than that of the parent and the transfectant cells (Table 7). The contrasts between the inflection points of SBC-3/GCS and SBC-3 cells disappeared following exposure to either 10 or 100 μM BSO.

Table 7: **Functions, second derivatives and inflection points for dose-response curves obtained from SBC-3 and SBC-3/GCS clonogenic survival assays ± BSO**

Cell line/Transfectant	f(x); f''(x)	Inflection points (µg/ml)
SBC-3	$f(x) = -2 + \frac{4}{1+\exp^{(-2.7+0.5x)}}$ $f''(x) = \frac{\left(\exp^{[-2.7+0.5x]}\right)^2}{\left(1+\exp^{[-2.7+0.5x]}\right)^3} - 0.81 * \frac{\exp^{(-2.7+0.5x)}}{\left(1+\exp^{[-2.7+0.5x]}\right)^2}$	(1) 3.1 µg/ml (2) 8.9 µg/ml
SBC-3 + 100 µM BSO	$f(x) = -2 + \frac{4}{1+\exp^{-2.50+0.57x}}$ $f''(x) = \frac{\left(\exp^{[-2.50+0.57x]}\right)^2}{\left(1+\exp^{[-2.50+0.57x]}\right)^3} - 0.94 * \frac{\exp^{(-2.50+0.57x)}}{\left(1+\exp^{[-2.50+0.57x]}\right)^2}$	(1) 2.1 µg/ml (2) 6.7 µg/ml
SBC-3/GCS	$f(x) = -2 + \frac{4}{1+\exp^{(-1.85+0.16x)}}$ $f''(x) = \frac{\left(\exp^{[-1.85+0.16x]}\right)^2}{\left(1+\exp^{[-1.85+0.16x]}\right)^3} - 0.10 * \frac{\exp^{(-1.85+0.16x)}}{\left(1+\exp^{[-1.85+0.16x]}\right)^2}$	(1) 3.4 µg/ml (2) 20 µg/ml
SBC-3/GCS + 10 µM BSO	$f(x) = -2 + \frac{4}{1+\exp^{(-2.58+0.49x)}}$ $f''(x) = \frac{\left(\exp^{[-2.58+0.49x]}\right)^2}{\left(1+\exp^{[-2.58+0.49x]}\right)^3} - 0.94 * \frac{\exp^{(-2.58+0.49x)}}{\left(1+\exp^{[-2.58+0.49x]}\right)^2}$	(1) 2.6 µg/ml (2) 8.0 µg/ml
SBC-3/GCS + 100 µM BSO	$f(x) = -2 + \frac{4}{1+\exp^{(-2.81+0.57x)}}$ $f''(x) = \frac{\left(\exp^{[-2.81+0.57x]}\right)^2}{\left(1+\exp^{[-2.81+0.57x]}\right)^3} - 1.29 * \frac{\exp^{(-2.81+0.57x)}}{\left(1+\exp^{[-2.81+0.57x]}\right)^2}$	(1) 2.6 µg/ml (2) 7.3 µg/ml

ii) Saos-2, Saos-2/p53- and Saos-2/p53 cells

A comparison of the inflection points in Saos-2 cells and its transfectants revealed less dramatic differences, where Saos-2 cells and Saos-2/p53- cells had comparable inflection points at low doses of cisplatin (Table 8). Their respective inflection points differed slightly, however, at higher doses. The biggest difference was found when the inflection points from these cell populations were compared to the inflections points obtained for Saos-2/p53 cells, particularly at high doses. Saos-2/p53 cells treated with high doses of cisplatin began the transition into the terminal (drug-resistant) plateau phase of the curve at a concentration of cisplatin almost 5 μg/ml higher than Saos-2 cells, and 2.5 μg/ml higher than Saos-2/p53- cells (Table 8).

Table 8: Functions, second derivatives and inflection points for dose-response curves obtained from Saos-2, Saos-2/p53- and Saos-2/p53 clonogenic survival assays

Cell line/Transfectant	f(x); f''(x)	Inflection points (μg/ml)
Saos-2	$f(x) = -0.66 + \frac{2.66}{1+\exp^{(-3.0+0.235x)}}$ $f''(x) = \frac{\left(\exp^{[-3.0+0.235x]}\right)^2}{\left(1+\exp^{[-3.0+0.235x]}\right)^3} - 0.15 * \frac{\exp^{(-3.0+0.235x)}}{\left(1+\exp^{[-3.0+0.235x]}\right)^2}$	(1) 7.13 μg/ml (2) 18.35 μg/ml
Saos-2/p53-	$f(x) = -0.972 + \frac{2.972}{1+\exp^{(-2.93+0.204x)}}$ $f''(x) = \frac{\left(\exp^{[-2.93+0.204x]}\right)^2}{\left(1+\exp^{[-2.93+0.204x]}\right)^3} - 0.082 * \frac{\exp^{(-2.93+0.204x)}}{\left(1+\exp^{[-2.93+0.204x]}\right)^2}$	(1) 7.91 μg/ml (2) 20.84 μg/ml
Saos-2/p53	$f(x) = -1.66 + \frac{3.66}{1+\exp^{(-2.86+0.18x)}}$ $f''(x) = \frac{\left(\exp^{[-2.86+0.18x]}\right)^2}{\left(1+\exp^{[-2.86+0.18x]}\right)^3} - 0.12 * \frac{\exp^{(-2.86+0.18x)}}{\left(1+\exp^{[-2.86+0.18x]}\right)^2}$	(1) 8.51 μg/ml (2) 23.05 μg/ml

Please note that the statistical comparison of the inflection points, although mathematically possible is not statistically appropriate, since this would involve the comparison of data that is already based on a non-linear regression analysis. The problem would be that this kind of analysis would take into account data that was already two degrees of separation from the measured phenomenon. Thus, the analyst would be conducting a statistical test on calculations derived from estimated data, and this degree of separation from the actual results is too wide to be reported with confidence. The interested reader should, however, make note that this comparison was conducted for the sake of academic interest, and the levels of significance supported the trends in favour of the changes hypothesized for both active and passive resistance mechanisms.

4. DISCUSSION

4.1 Summary

To summarise the key points of our results pertaining to the Saos-2 cell line and its transfectant, Saos-2/p53 (and Saos-2/p53-), the expression of the transfected p53 genes in Saos-2/p53 cells have been confirmed by western blot. p53 has also been found to have an effect on the cell cycle that appears to be consistent with its function. The presence of p53 in the Saos-2 cells had an effect the shape of dose-response curves consistent with the hypothesis effects of passive drug resistance, where the surviving fraction of the clonogenic population in the Soas-2/p53 cells was significantly reduced when compared to the surviving fraction of the parent Saos-2 population, or the Saos-2/p53- population. Reversal the p53 transfection (where Saos-2/p53 cells expressing p53 protein were reduced to below detectable levels) resulted in a return of the dose-response curve shape in the transfectant to that seen in the parent cell line, which would indicate an increase in passive resistance. Furthermore the lack of wild-type p53 resulted in an increased number of cells surviving at the terminal plateau. Reversal of this resistance (i.e. by the addition of a w/t p53 gene) resulted in a significantly lower proportion of cells surviving at high doses.

To summarise our results pertaining to the SBC-3 cell line and its transfectant, SBC-3/GCS, the expression of the transfected γ-GCS genes have been confirmed by western blot, and the presence of higher levels of γ-GCS in the SBC-3/GCS cell line has been conformed by GSH quantification. The transfection of γ-GCS into SBC-3/GCS had

effects on the shape of dose-response curves consistent with the hypothesis of active drug resistance, where the increased expression of GSH resulted in an increase in the shoulder of the curve, and the end of the shoulder indicated an overwhelming of the GSH protective mechanism. Partial/complete inhibition of γ-GCS via exposure to BSO resulted in a decrease in this shoulder, which again would be consistent with the hypothesis that the decreased presence of GSH inhibited its ability to protect the cell against the cytotoxic effects of cisplatin.

4.2 Western Blotting

In the case of the western blotting assay, Saos-2 cells did not reveal detectable levels of p53. Saos-2/p53 cells had detectable levels of p53, and produced high levels of the gene product, with a statistically significant increase in the relative intensity of the p53 band in Saos-2/p53 cells following induction by IPTG (Figure 5). Furthermore, we demonstrated that exposure of the cells to IPTG did not in itself account for the p53 band, since exposure of Saos-2 cells to IPTG had no effect on the western blot assay. Since a lack of a factor necessary for a drug to exert its cytotoxic effects on a cell line is the base criteria for a passive resistance mechanism, the absence of p53 in the parent Saos-2 cells, and the confirmed presence of p53 in Saos-2/p53 cells, provided an excellent model to explore the concept of passive resistance.

The transfection of γ-GCS resulted in high levels of expression of the gene product, with an increase in the relative intensity of the bands of interest (Figure 5). These differences were statistically significant, where the SBC-3/GCS transfectant had a

greater than 2-fold increase in GSH when compared to the parent cell line, even following exposure to CP (Table 3). That GSH levels dropped following exposure to CP in both cell lines is to be expected, since CP would be conjugated to GSH, and exported via active transport of glutathione conjugates (Kurokawa *et al.*, 1995). Exposure to BSO, a known inhibitor of γ-GCS, also lowered GSH levels as expected (Table 4; Figure 9A). Although strong inhibition of GSH synthesis was observed in the parent SBC-3 cell line following exposure to 10 μM BSO, higher levels of GSH were still detected in the transfectant at the same concentrations of BSO (Table 4; Figure 9B). At 100 μM concentrations of BSO, GSH levels in both the parent and the transfected cell populations were found to be roughly equivalent, indicating an extensive inhibition of GSH synthesis. The presence of an extra copy of γ-GCS (in this case due to transfection) as detected in the western blot, is further supported by these data, and would be also consistent with a natural gene amplification event. Note that gene amplification is one of the means by which our concept of active resistance can be achieved.

4.3 Flow Cytometry

4.31 Saos-2 cells and their transfectants

Flow cytometry yielded strong support in demonstrating the effects of p53. Both Saos-2 and the transfectant Saos-2/p53 cell population had very similar profiles prior to CP exposure (Table 1; Figure 7), although the slightly higher percentage of Saos-2/p53 cells found in $G1/G_0$ would be indicative of cell cycle arrest, which could be associated with functional p53 protein. Although high levels of p53 are produced in this transfectant

following a 24-hour exposure to IPTG (Figure 5), basal levels of p53 are still produced as the double-vector lacSwitch system used in this cell line is "leaky" even in the absence of induction (Wang *et al.*, 1998). The leaky nature of this system was in fact especially useful, where low, non-induced levels of p53 were sufficient to cause sensitization of the transfectant to CP, as seen in the clonogenic assay (Figure 10). Further sensitization of Saos-2/p53 cells by induction of high levels of p53 might intuitively serve to further decrease the number of cells surviving at high doses. Wang *et al.* (1998) have, however, conducted clonogenic studies on induced Saos-2/p53 cells and did not report any appreciable change in cell death. These authors did not conduct their dose-response assays using the wide dose-ranges we have used in our methodology, and thus future investigation into this area might prove to be promising.

The presence of "leaky" levels of p53 in the Saos-2 transfectants facilitated our analysis, as induction of high levels of p53 resulted in G_0/G_1 cell cycle arrest (Figure 7). Consistent with the effects of p53 on the cell cycle, transfectants exposed to CP showed a much higher percentage of cells in $G1/G_0$, with a correspondingly low proportion of cells being found in the S- or G2/M-phases (Figure 7 E, F). This differed dramatically from parent Saos-2 cells, where the majority of the cell population was found to be predominantly in the S-phase (Table 1; Figure 7 B). This might be explained in that the lack of p53 may result in the cell being unable to undergo G1 arrest, where p53 has been shown to mediate cell cycle arrest following exposure to DNA-damaging agents (Chang *et al.*, 1999). Recently, p53 was implicated in transition-coupled repair, which is a form of nucleotide excision repair that occurs more rapidly in the transcribed strands of active

genes than in the remainder of the genome (McKay, Ljungman & Rainbow, 1999). Although information in this area is scarce, it is possible that p53-deficient cells attempt to synthesize damaged DNA during the S-phase and become slowed down or arrested in various stages of that phase, where wild-type p53 has been proposed to enhance recovery of transcription following damage to DNA (McKay and Ljungman, 1999). This phenomenon might occur as a function of the cell's inability to synthesize DNA past damaged points, due to a deficient nucleotide excision repair mechanism, where cells that are repair deficient have been found to accumulate in the S-phase (personal communication with Dr. Bruce MacKay, Ottawa Regional Cancer Centre).

By exposing Saos-2/p53 cells to 5 mM concentrations of IPTG for several weeks at a time, it was possible to eliminate most p53-containing cells from the population, as indicated by the lack of detectable p53 in the western blot (Figure 5). These Saos-2/p53- cells shared a similar cell cycle distribution profile with that of Saos-2 parent cells, further supporting the contention that the cells that comprised that population were not expressing p53 (Figure 7 C,D).

4.32 SBC-3 cells and their transfectants

SBC-3 cells exposed to CP had an increase in the number of cells in G2/M (Table 2; Figure 8 B). Of particular interest, however, is that, while parent and GCS-transfected cells shared a similar profile prior to CP exposure (Figure 8 A vs. C), the transfected population was able to maintain a roughly similar proportion of cells in G1 while the parent cell line was not (Figure 4 B vs. D). While these changes were slight, it might be

indicative of the increased ability of SBC-3/GCS cells to inactivate CP before it can exert a cytotoxic effect and induce a cellular response. Certainly in this capacity it provides an indication that the transfection of an extra copy of γ-GCS may provide a chemoprotective effect.

4.4 The signficance of reversing the effects of transfection in both Saos-2 and SBC-3 cells

An examination of Saos-2 cells, SBC-3 cells, and their transfectants via western blotting, GSH quantification, and flow cytometric analysis was conducted with the objective of confirming the presence/absence of the genes of interest. These data also verified that, when present, the resultant gene products would influence the response of the cell to cytotoxic stimuli in a predictable way. By inhibiting the formation of the gene products (as was the case with BSO-inhibition of GSH in the SBC-3 cell line), or the effective elimination of p53 expressing Saos-2 transfectants (by chronic exposure of the transfectants to IPTG) , we were able to effectively reverse the effects of transfection in the respective cells. In all cases, this manipulation resulted in a return to the responses observed in the parent cells, and suggested that the various changes we saw in the transfectants following CP exposure was a function of the transfected gene products, and not due to other random variables. The confidence gained via this in-depth analysis of the transfectants permitted us to closely scrutinize the effects of transfection on the dose-response curve, and also supported the contention that any observable changes were attributable to the effects of the transfection.

4.4 Clonogenic analysis of the cell lines

4.41 The suitability of the clonogenic assay

Before discussing the results of the clonogenic assay, it may be useful to first explain its suitability in our analysis. There are numerous assays available to investigate cytotoxicity *in vitro*, however, the method that we selected was the clonogenic assay. Most other methods (such as 3-[4,5-Dimethylthiazol-2-y]-2,5-diphenyltetrazolium bromide; thiazoyl blue (MTT), 2,3-bis[2-Methoxy-4-nitro-5-sulfophenyl]-2,5-diphenyltetrazolium-5-carboxanilide (XTT)) and/or trypan blue staining are based on particular aspects of cellular physiology. For instance, both the XTT and the MTT methods measure the functioning of cellular reducing enzymes (Lamontagne *et al.*, 1994) and trypan blue measures the viability of cell membranes (Cole, 1986). It is quite possible for cells to be in a repair state, and still capable of subsequent division in spite of damage to their enzymatic systems, resulting in an erroneous negative estimation. Conversely, cells that have died might still contain functioning enzymes, resulting in a falsely positive measurement. These problems are eliminated through the use of the clonogenic assay, which assesses cellular health as a function of the ability of single cells to form colonies. The percentage of live colonies relative to a drug-free control is determined following an incubation period, and the duration of incubation depends on the cell line being used.

4.42 Saos-2 cells and their transfectants

In the case of Saos-2 cells, the dose response curve was found to end with an elevated terminal plateau, containing 0.17% of the cell population (Table 5; Figure 10). Although this figure may appear to be small, it is extremely relevant in a clinical sense, since these cells could rapidly proliferate and would be much more resistant to subsequent courses of chemotherapy. Soas-2/p53 cells, however, displayed a considerably smaller percentage of cells surviving at the terminal plateau phase (0.09%), with a steeper slope (Table 5; Figure 10), suggestive that even the percentage of cells surviving at the terminal plateau might be further reduced at a slightly higher dose. A return to the parent dose-response profile was noted in the Saos-2/p53- cells, although the percentage of cells surviving at the terminal plateau was slightly lower than that of the parent, possibly indicative of the residual presence of p53-transfected cells in the population that were not detectable on the western blot (Table 5; Figure 10). The observation that cisplatin was capable of killing a proportion of the Saos-2 parent cells (which lack p53) indicates that cisplatin kills cells by both p53-dependant and p53-independent mechanisms. Also noted was that the dose-response curves for Saos-2/p53 cells still possessed a terminal, albeit much reduced, plateau. Based on our hypothesis, this would be consistent with the presence of an additional mechanism of saturable passive resistance. Of note is that a shoulder at low doses was observed in Saos-2, Saos-2/p53 and Saos-2/p53- cells, and is also indicative of mechanisms of active resistance at work in the cell line (Figure 10). The shape and location of the shoulder did not change, however, across the cell line and can thus be assumed to not have an impact on the changes in the terminal plateau that we observed with respect to p53 transfection.

4.43 SBC-3 cells and their transfectants

Based on the hypothesis of active resistance, one would expect an increase in the LD_{50} subsequent to gene amplification, resultant from a right shift of the dose-response curve. This is supported by our data in that the increased presence of GSH results in a right-shift of the curve (Figure 11 inset), and the point of inflection shifts from 3.1 μg/ml to 3.4 μg/ml for the transfectant (Table 7). Another marked change, however, occurs in the SBC-3/GCS dose-response curve, where the slope becomes much more shallow when compared to the slope of the parent cell line (Table 6). The effect of this change in slope is quite pronounced and warrants further discussion.

4.44 The change in the slope of the dose-response curves found in SBC-3/GCS cells (± BSO), when compared to SBC/3 cells (± BSO)

Based on our concept of active resistance, increased levels of GSH would serve to more completely inactivate CP at doses similar to that administered to a cell line that produced lower levels of GSH. The result would be similar to that of the competitive inhibition of a drug, where the entire dose-response curve would be right-shifted, and more drug would be required to bind to its molecular target. A concurrent change in the slope, however, would indicate that another, possibly secondary, mechanism might also be exerting an effect on the dose-response curve, resulting in a greater net increase in resistance. There are several possibilities that may account for this additional mechanism of secondary resistance. One possibility would be an increase in the intracellular pH as a

function of the relationship between CP and GSH. It has been reported that GSH levels drop drastically following a decrease in intracellular pH (Ikebuchi *et al.*, 1993; Koyama *et al.*, 2000) and it is possible that this may occur during toxic insult at high doses. This response could be due to an overwhelming of the antioxidant potential of GSH, where higher levels of GSH result in an enhanced ability of the cell to maintain a stable and higher physiological pH. This would be consistent with the observation that the optimal pH for γ-GCS activity is 8.2 (personal communication with Dr. Owen Griffith, University of Michigan). It is also well documented that CP cytotoxicity is enhanced at lower pH (Laurencot & Kennedy, 1995). This characteristic has been investigated in regards to the biomodulation of CP using acetazolamide, a carbonic anhydrase inhibitor, with a resultant increase in cytotoxicity (Teicher *et al.*, 1993). The possible sources for enhanced toxicity of CP at low pH have also been investigated, and it is suggested that CP-DNA adduct formation is increased (Atena *et al.*, 1993; Laurencot & Kennedy, 1995), where higher intracellular pH has been associated with a reduction of CP binding to molecular targets (Chau, 1999). The accumulation of CP within the cell at low pH may also occur as a function of altered efflux via H^+-sensitive active transport mechanisms, and may result in ion trapping, sequestering CP within the cell (Atena *et al.*, 1993; Chau, 1999), where cisplatin has recently been reported to decrease the activity of ATP-driven H^+ pumps in the cell membrane (Shiraishi et al., 2000). Thus, although the aquation of cisplatin within the cytoplasm may not directly increase hydrogen ion concentration, the ability of cisplatin to decrease ATP-dependant H^+ pump activity (and thus decrease the extrusion of hydrogen ions to the extracellular matrix) may indeed result in a decrease in intracellular pH at high doses. Furthermore, low intracellular pH has been implicated in a

slowing or inhibition of cellular proliferation due to a decrease in protein synthesis, which may decrease cellular sensitivity to CP during drug exposure (Atena *et al.*, 1993). All of these factors might thus account for the change in slope observed in the dose-response curve of SBC-3/GCS cells exposed to CP, provided that high levels of GSH increase intracellular pH. In this case, the antioxidative potential provided by higher levels of GSH might offset any decrease in pH that would otherwise result in the trapping of CP and an increase in its toxicity. High levels of GSH might also indirectly prevent DNA-adduct formation via the maintenance of a higher pH, *in addition* to directly assisting in its elimination via conjugation and its consequent inactivation. This suggestion is supported by our data in that inhibition of the parent (SBC-3) cell line using BSO results in an increase in the steepness of the slope of the dose-response curve, and this trend is consistent in SBC-3/GCS cells inhibited by BSO as well (Table 6, Figure 13). Both a change in dose-response curve slope and cisplatin resistance mechanisms based on alterations of pH would be consistent with non-saturable passive resistance. Hence, our studies did support changes in keeping with active resistance (i.e. a shift of the shoulder of the dose-response curve to the right) when GSH production is increased, but also raised the intriguing possibility that GSH may confer increased resistance to cisplatin by important but previously unrecognized mechanisms in addition to simple binding and inactivation of cisplatin.

Other explanations for the change in slope of the dose-response curve might involve the effects specific to the presence of two or more γ-GCS genes performing the

same function in the SBC-3/GCS cells line. Possible reasons for the decreased slope found in the dose response curve in this system might include:

1. That a dual copy of γ-GCS not only increases the quantity of intracellular GSH, but also increases the ability of GCS to produce GSH following rapid depletion by CP-GSH adduct formation.

2. That the presence of more than one copy of γ-GCS further influences intracellular pH.

3. That the increased production of GSH in SBC-3/GCS cells influences other resistance mechanisms that are related to GSH synthesis

A dual copy of γ-GCS increases the ability of GCS to produce GSH following rapid depletion

During the *in vitro* exposure of SBC-3/GCS cells to CP, intracellular pools of GSH are consumed in the formation of GSH-CP adducts and an increased demand is placed on the GSH synthesis system. In a single copy enzyme system, as the demand increases, the output of the γ-GCS is increased (where high levels of GSH act as negative feedback loop), until it reaches its maximal rate. At maximal GSH production, this active resistance mechanism becomes overwhelmed and theoretically at this point the shoulder of the D-R curve would end and percent clonogenic survival would decrease rapidly.

In the case of the transfection of γ-GCS, there are (at least) two functional copies of the enzyme performing the same work. Since the production of GSH is regulated by the feedback inhibition of GCS, one would expect that both of these enzymes are induced in concert during GSH depletion. Thus, the formation of GSH might occur twice as rapidly when compared to the single copy enzyme system. In such a case, this system would not only be capable of creating more GSH to complex with CP, but would also be capable of replenishing the GSH pool more rapidly. Thus, as CP concentrations increase, the γ-GCS system of SBC-3/GCS cells would be capable of responding more rapidly than a "single copy" system. This increased GSH synthetic ability may translate into the increased survivability of transfected cells at higher concentrations, with the increased kinetics of a "twin-enzyme" system be represented by a slower decline in the slope of the DRC. The twin-enzyme system might therefore resist the chemotherapeutic onslaught of CP more completely at lower concentrations, but would inevitably become overwhelmed at highly cytotoxic levels.

The presence of more than one copy of γ-GCS further influences intracellular pH

Another possible mechanism to account for the decreased slope in GCS-transfected cells is that these cells contain extra copies of γ-GCS, and are hence able to exert a stronger influence on intracellular pH during the escalating exposure to CP. If this were correct, and the assumption of the intracellular pH on γ-GCS activity and the cytotoxicity of CP were correct, then the pH of γ-GCS-transfected cells would decline less rapidly during exposure to CP. This resistance to decreases in intracellular pH would have the effect of reducing the cytotoxicity of CP in a manner related to the quantity of

intracellular γ-GCS, This relationship would, in turn decrease the slope of the clonogenic dose-response curve.

The increased production of GSH in SBC-3/GCS cells influences other resistance mechanisms that are related to GSH synthesis

Kurokawa *et al.*, 1995 demonstrated that the transfection of γ-GCS not only increased intracellular levels of GSH as we have demonstrated, but was also related to an increase in GS-X pump activity. The increased efflux of GSH-conjugates (including conjugated CP) in SBC-3/GCS cells via the GS-X pump might thus function as a mechanism of secondary resistance that could become overwhelmed at higher doses of CP. The presence of different, but related, resistance mechanisms might thus account for the shallow slope of the dose-response curve in the case of the γ-GCS transfected cells. The change in the steepness of the slope during inhibition with BSO provides further evidence that this change in slope is due to a γ-GCS-related event.

Other mechanisms indirectly related to GSH synthesis might also play a role in the increased resistance of SBC-3/GCS cells to cisplatin. For instance, it is widely reported that GSH rapidly reacts with reactive intracellular electrophiles such as hydrogen peroxide (Griffith & Mulcahy, 1999). This function plays a critical role in the protection of mitochondria, where high levels of H_2O_2 are produced as a consequence of oxidation, and recently the ability of GSH to protect mitochondria from the harmful effects H_2O_2 was also implicated in the regulation of apoptosis (Hall, 1999). Another

investigator has also reported that H_2O_2 secretion is increased in human monocytes exposed to CP (Pai & Sodhi, 1991). If this phenomenon is applicable to other cell types, it is possible be that the harmful effects of increased H_2O_2 secretion as a function of CP exposure is significantly decreased in cells that concurrently express higher levels of GSH, indicating a complex interrelationship that might be expressed by a change in slope on the dose-response curve.

Thus, although the change in slope is not directly supported by our hypothesis, it could be accounted for in a way that would be indicative of the presence of a secondary resistance mechanism, in addition to the chemoprotective effect of increased GSH production. If our hypothesis were valid, this would be a perfect example of how our approach might be used in order to facilitate the discovery of a new resistance mechanism, where GSH production may confer non-saturable passive resistance or "less-saturable" active resistance.

4.5 The applicability of our observations and conclusions

Our observations and analyses provide support for the hypothesis of the relationship between dose-response curve shapes and active vs. passive resistance. The potential advantages in being able to classify a particular mechanism in this sense include that it could be of value in the assessment of biomodulatory strategies, and may provide a new dimension in the discovery of new agents. Since a relationship between the shape of the dose-response curve and specific mechanisms of resistance has been established, it would now be beneficial to examine this relationship with a cell line transfected with

various drug resistance mechanisms. Subsequent exposure to many different antineoplastic agents would also allow the construction of a drug-response profile relative to various resistance mechanisms. Once the dose-response profile has been found for each drug-resistance mechanism and each compound, possible synergy between these factors could be determined using non-linear regression modelling. This method could set a precedent for a completely new philosophy in drug development and testing, in addition to the clinical benefit of biomodulation based on the dose-response relationship.

5. REFERENCES

1. Andrews, P.A. (1994). Mechanisms of acquired resistance to cisplatin. In: Anticancer drug resistance. Eds. Goldstein, L.J. and Ozols, R.F. Kluwer Academic Publishers, New York. pp. 217-248.

2. Ahmad, S, Okine, L., Wood, R. (1987). γ-glutamyl transpeptidase (γ-GT) and maintenance of thiol pools in tumour cells resistant to alkylating agents. Journal of Cell Physiology 131: 240-246..

3. Arrick, B.A., and Nathan, C.(1984). Glutathione metabolism as a determinant of therapeutic efficacy: A review. Cancer Research 44: 4224-4232.

4. Atena, A., Burrman, K.J., Noteboom, E. and Smets, L.A. (1993). Potentiation of DNA-adduct formation and cytotoxicity of platinum-containing drugs by low pH. International Journal of Cancer 54: 166-172.

5. Beck, W.T. and Dalton, W.S. (1997). Mechanisms of drug resistance. In Principles and Practice of Oncology (Ch. 19.11). 5th ed. Eds. Dwita, V.T., Hellman, S. and Rosenberg, S.A. Lippincot-Raven Publishers, New York, pp.498-509.

6. Beutler, B., Gelbart, T., Kondo, T. and Matsunaga, A.T. (1999). The molecular basis of a case of γ-glutamylcysteine synthetase deficiency. Blood 94(8): 2890 - 2894.

7. Chang, D., Chen, F., Zhang, F., McKay, B.C. and Ljungman, M. (1999). Dose-dependent effects of DNA-damaging agents on p53-mediated cell cycle arrest. Cell Growth and Differentiation 10: 155-162.

8. Chau, Q., Stewart D.J. (1999). Cisplatin efflux and binding in the HTB56 human lung adenocarcinoma cell and the E-8/0.7 cisplatin-resistance variant. Cancer Chemotherapy and Pharmacology 44: 193-202.

9. Chen et al., P., Chen et al., Y., Bookstein, R and Lee, W. (1990) Genetic mechanisms of tumour suppression by the human p53 gene. Science 250: 1576-1579.

10. Cole, S.P.C. (1986). Rapid chemosensitivity testing of human lung tumour cells using the MTT assay. Cancer Chemotherapy and Pharmacology 17: 259-263.

11. Colvin, O.M., Friedman, H.S., Gamcsik, M.P., Fenselau, C and Hilton, J. (1993). Role of glutathione in cellular resistance to alkylating agents. Advances in Enzyme Regulation 33: 19-26.

12. Fardel, O. Lecureur, V. and Guillouzo, A. (1996) The p-glycoprotein multidrug transporter. General Pharmacology 27(8): 1283-1291.

13. Freshney, R.I. (1994). Quantitation and Experimental Design. In: Culture of Animal Cells: A manual of basic techniques (3rd ed.), Wiley-Liss, New York. pp. 278-279.

14. Gilbert, H.F. (1990). Molecular and cellular aspects of thiol-disulfide exchange. Advances in Enzymology and Related Areas of Molecular Biology 63: 69-172.

15. Griffith, O.W. (1999). Biologic and pharmacologic regulation of mammalian glutathione synthesis. Free Radical Biology and Medicine 27(9-10): 922-935.

16. Griffith, O.W., and Friedman, H.S. (1991). In synergism and antagonism in chemotherapy. Eds. Chau, T.C. and Rideout, P.C. Academic press, San Diego. pp. 285-299.

17. Griffith, O.W. and Mulcahy, R.T. (1999). The enzymes of glutathione synthesis: γ-glutamylcysteine synthetase. In: Advances in Enzymology and related areas of molecular biology (vol. 73). Ed: Purich, D.L. John Wiley & Sons, New York, ISBN 0-471-24644-1

18. Hall, A.G. (1999). The role of glutathione in the regulation of apoptosis. European Journal of Clinical Investigation 29: 238-245.

19. Higashi, T., Tateishi, N., Naruse, A., Sakamoto, Y. (1977). Rat liver glutathione: possible role as a reservoir of cysteine. Journal of Nutrition 107: 51-60.

20. Ikebuchi, M., Kashiwaga, A., Asahina, T., Tanaka, Y., Takagi, Y., Nisio, Y., Hidaka, H., Kikkawa, R., and Shigeta, Y. (1993). Effect of medium pH on glutathione redox cycle in cultured human umbilical vein endothelial cells. Metabolism 42: 1121-1126.

21. Inoue, Y., and Kimura, A. (1995). Methylglyoxal and regulation of its metabolism in microorganisms. Advances in Microbiological Physiology 37: 177-227.

22. Keppler D., Leier, I. And Jedlitschky, G. (1997) Transport of glutathione conjugates and glucuronides by NDR proteins MRP1 and MRP2. Biological Chemistry 378(8): 787-791.

23. Kinsella, A.R., Smith, D. and Pickard, M. (1997) Resistance to chemotherapeutic anti-metabolites: a function of salvage pathway involvement and cellular response to DNA damage. British Journal of Cancer 75(7): 935-945.

24. Koivusalo, M., Baumann, M. and Uotila, L. (1989). Evidence for the identity of glutathione-dependent formaldehyde dehydrogenase and class III alcohol dehydrogenase. FEBS Letter 257: 105-109.

25. Komiya et al., T., Hirashima, T. and Kawase, I. (1999) Clinical Significance of p53 in non-small cell lung cancer. Oncology Reports 6: 19-28.

26. Koyama Y., Kimura, Y., Hashimoto, H., Matsuda, T., and Bada, A. (2000). L-lactate inhibits L-cystine/L-glutamate exchange transport and decreases glutathione content in rat cultured astrocytes. Journal of Neuroscience Research 59: 685-691.

27. Kurokawa, H., Ishida, T., Nishio, K., Arioka, H., Sata, M., Fukumoto, H., Miura, M. and Saigo, N. (1995). γ-glutamylcysteine synthetase gene overexpression results in increased activity of the ATP-dependent glutathione-conjugate transport pump, and cisplatin resistance. Biochemical and Biophysical Research Communications 216: 258-264.

28. Lai, G., Ozols, R.F., Young, R.C., Hamilton, T.C. (1989). Effects of glutathione on DNA repair in cisplatin-resistant human ovarian cancer cell lines. Science 81(7): 535-539.

29. Lamontagne, P., Maion, G and Page, M. (1994). Cytotoxicity testing using a soluble tertazolium formazin derivative. Cellular Pharmacology 1: 191-174.

30. Laurencot, C.M. and Kennedy, K.A. (1995). Influence of pH on the cytotoxicity of cisplatin in EMT6 mouse mammary tumour cells. Oncology Research 7: 371-379.

31. MacKay, B.C., Ljungman, M. and Rainbow, A.J. (1999). Potential roles for p53 in nucleotide repair. Carinogenesis 20: 1389-1396.

32. MacKay, B.C., and Ljungman, M. (1999). Role for p53 in the recovery of transcription and protection against apoptosis induced by ultraviolet light. Neoplasia 1: 276-284.

33. Meister, A. (1995). Glutathione Metabolism. In: Methods in enzymology: Biothiol Part A (vol. 251). Ed. Packer, L. Academic Press, New York. pp.1-30.

34. Meister, A., and Griffith, O.W. (1979). Effects of methionine sulfoximine analogs on the synthesis of glutamine and glutathione: Possible chemotherapeutic implications. Cancer Chemotherapy Reports 63: 1115-1121.

35. Mulcahy, R.T., Bailey, H.H., and Gipp, J.J. (1995). Transfection of complementary DNAs for the heavy and light subunits of human γ-glutamylcysteine synthetase results in an elevation of intracellular glutathione and resistance to melphalan. Cancer Research 55: 4771-4775.

36. Nassim, M.A., Rouini, M.R., Cripps, M.C., Shirazi F.H., Veerasinghan, S., Molepo, J.M., Obrocea, M., Redmond D., Bates, S., Fry, D., Stewart D.J., and Goel, R. (1998a) Effects of PALA on the pharmacokinetics of 5-Fluorouracil. Oncology Reports. 5: 217-221.

37. Nassim, M.A., Dulude, H., Goel, R., and Stewart, D.J. (1998). In vitro additive and sub-additive effects of chemotherapeutic drug combinations in human lung

adenocarcinoma (HTB-56) cells. Proceedings of the American Association of Clinical Oncology vol. 17: abstract 952.

38. Nassim, M.A., Goel., R., and Stewart, D.J. (1997). Potential Implications of dose-response curve shapes for chemotherapeutic drugs in HTB-56 cells. Proceedings of the American Association for Cancer Research vol. 38: abstract 2075.

39. National Cancer Institute of Canada. (2000). Canadian cancer statistics 2000. Toronto, Canada.

40. O'Brien, N.L., and Tew, K.D. (1996). Glutathione and related enzymes in multidrug resistance. European Journal of Cancer 32A: 967-978.

41. O'Dwyer, P.J., Hamilton, T.C., Yao, K.S., Tew, K.D., and Ozols, R.F. (1995). Modulation of glutathione and related enzymes in reversal of resistance to anticancer drugs. Hematology-Oncology Clinics of North America 9:383-396.

42. Ogreteman, B., Bahadori, H., McCauley, M., Baylan, A., Green, M., and Safa, A.R. (1989). Lack of correlation of MRP and γ-GCS overexpression with doxorubicin-resistance due to increased apoptosis in SV40 large T-antigen-transformed human mesothelial cells. Cancer Chemotherapy and Pharmacology 42: 441-446.

43. Okaichi, K., Wang, L., Ihara, M. and Okamura, Y. (1998). Sensitivity to ionizing radiation in Saos-2 cells transfected with mutant p53 genes depends on the mutation position. Journal of Radiation Research 39: 111-118.

44. Ormerod, J.P., Orr, R.M. and Peacock, J.H. (1994). The role of apoptosis in cell killing by cisplatin: A flow cytometric study. British Journal of Cancer 69: 93-100.

45. Pai, K. and Sodhi, A. (1991). Effect of cisplatin, rIFN-Y, LPS and MDP on release of H2O2, O2- and lysozyme from human monocytes in vitro. Indian Journal of Experimental Biology. 29(10): 910-915.

46. Perez, R.P. (1998) Cellular and Molecular Determinants of Cisplatin Resistance. European Journal of Cancer. 34(10): 1525-1542.

47. Raaphorst, G.P., Yang, D.P., Grewaal, D., Stewart, D.J., Goel, R. and Ng, C.E. (1995). Analysis of mechanisms of cisplatin resistance in 3 pairs of human tumour cell lines expressing normal and resistant responses to cisplatin. Oncology Reports 2: 1037=1043.

48. Redmond, S.M.S., Joincourt, F., Buser, K., Zeimeicki, A., Altermatt, H.J., Fey, M., Margison, G. and Cerny, T. (1991). Assessment of p-glycoprotein, glutathione-based detoxifying enzymes and O^6-alkylhguanine-DNA-alkyltransferase as potential

indicators of constitutive drug resistance in human colorectal tumours. Cancer Research 51: 2092-2097.

49. Roth, J.A. and Cristiano, R.J. (1997) Gene therapy for cancer: what have we done and where are we going? Journal of the National Cancer Institute 89(1): 21-39.

50. Schmitt, C.A. and Loew, S.W. (1999) Apoptosis and Therapy. Journal of Pathology 187(1): 127-137.

51. Schröder, C.P., Godwin, A.K., O'Dwyer, P.J., Tew, K.D., Hamilton, T.C. and Ozols, R.F. (1996). Glutathione and drug resistance. Cancer Investigation 14: 158-168.

52. Sheikh, M.S. and Fòrnace Jr., A.J. (2000). Role of p53 members in apoptosis. Journal of Cellular Physiology 182: 171-181.

53. Shen, H., Kauvar, L., and Tew, K.D. (1997). Importance of glutathione and associated enzymes in drug response. Oncology Research 9: 295-302.

54. Shiraishi, Y., Nagai, J., Murakami, T., and Takano, M. (2000). Effect of cisplatin on H+ transport by H+ - ATPase and Na+/H+ exchanger in rat renal brush-border membrane. Life Sciences 67(9): 1047-1058.

55. Sies, H. (1999). Glutathione and its role in cellular function. Free Radical Biology and Medicine 27(9/10): 916-921.

56. Soltaninassab, S.R., Sekhar, K., Meredith, M.J., Freeman, M.L. (2000). Multifaceted regulation of γ-glutamylcysteine synthetase. Journal of Cellular Physiology 182: 163-170.

57. Stewart, D.J., Dahroude, S., Banerjee, S., Tomiak, E. and Donker, R. (2000). Clinical dose-response relationships in non-small cell lung cancer: Implications for resistance mechanisms and resistance modulation. Proceedings of the American Association for Cancer Research 41: 4401.

58. Stewart, D.J., Raaphorst, G.P., Yau, J. and Beaubien, A. (1996). Active vs. passive resistance, dose-response relationships, high-dose chemotherapy, and resistance modulation: A hypothesis. Investigational New Drugs 14: 115-130.

59. Tateishi, N., Higashi, T., Narure, A., Nakashima, K., Shiazaki, H., Sakamoto, T. (1977). A novel physiological role of liver glutathione as a reservoir of L-cysteine. Journal of Biochemistry 90: 1063-1610.

60. Teicher, B.A., Liu, S.D., Liu, J.T., Holden, S.A. and Herman, T.S. (1993). A carbonic anhydrase inhibitor as a potential modulator of cancer therapies. Anticancer Research 13: 1549-1556.

61. Tew, K.D., Monks, A., Barone, L., Rosser, D., Akerman, G., Montali, J.A., Wheatley, J.B., Schmidt Jr., D.E. (1996). Glutathione-associated enzymes in the human cell lines of the National Cancer Institute Drug Screening Program. Molecular Pharmacology 50: 149-159.

62. Volm, M. (1998) Multidrug resistance and its reversal. Anticancer Research 18: 2905-2918.

63. Wang, L.H., Okaichi, K., Ihara, M. and Okamura, Y. (1998). Sensitivity of anticancer drugs in Saos-2 cells transfected with mutant p53 varied with mutation point. Anticancer Research 18: 32-36.

64. Yan, N. and Meister, A. (1990). Amino acid sequence of rat kidney γ-glutamylcysteine synthetase. Journal of Biological Chemistry 265 (3): 1588-1593.

65. Zeigler, D.M., (1985). Role of Reversible oxidation-reduction of enzyme thiol-disufides in metabolic regulation. Annual Review of Biochemistry 54: 305-329.

66. Zhang, G., Kimijima, I., Tsuchiya, A. and Abe, R. (1998) The role of bcl-2 expression in breast carcinomas. Oncology Reports 5: 1211-1216.

67. Zhang, K., Mack, P. and Wang, K.P. (1998) Glutathione-related mechanisms in cellular response to anticancer drugs. International Journal of Oncology 12: 871-882.